Peer Review File

Manuscript Title: The role of NSP6 in the biogenesis of the SARS-CoV-2 replication organelle

Reviewer Comments & Author Rebuttals

Reviewer Reports on the Initial Version:

Referees' comments:

Referee #1 (Remarks to the Author):

This manuscript investigates the role of the viral non-structural transmembrane proteins of SARS-CoV-2 (NSP6) in regulating the properties of the Nsp3/4-dependent replication organelle (RO) in tissue culture cells. This is an exciting question and timely subject. I think this story has great potential but some major points need to be addressed below.

Conclusions drawn from the data are that (N-term tagged) NSP6 drives formation of what appears to be a round NSP6 compartment by FM and a flat zippered ER cisternal compartment by immuno-EM. Both of which are near to NSP3/4 ROs. They show that the NSP6-dependent zippered ER membranes seen by EM are close to NSP3/4-dependent ROs and that exogenous expression of NSP6 will increase the abundance of these ROS. Thus there appears to be a link between NSP6 ER domains and NSP3/4 Ros even though they are non-overlapping. However, it baffles me why the flat zippered ER structures that NSP6 forms by EM are completely different in shape from the round structures imaged using FM. This needs to be resolved or explained. For example, an endosome has the same shape by FM that it does by EMT. Have the authors excluded whether the tagged NSP6 zippers some ER but the round structures seen by FM are NSP6 being degraded by lysosomes/endosomes?

By FM, NSP6 labeled compartments exclude luminal proteins but contain some membrane proteins. But what happened to the ER in these pictures? Why would ER proteins now only label blobs and no longer label the rest of the ER? I can't tell if these cells were just over transfected. This is also relevant to the FRAP analysis, the NSP6 compartments slowly recover membrane proteins and poorly recover "immobile" NSP6, but I'm not sure what these compartments are because the VAP labelled membranes are not normal ER anymore. Again, looks more like autophagy or a lysosome. Notably a 3 AA deletion (AA106-108) in NSP6 is found in four variants of concern. This leads to the interesting question of how does this deletion alter NSP6 behavior. They probe its solubility (fig 2m), its localization to NSP6 domains vs. general ER (fig 2o) and its ability to form NSP6 compartments (fig 2l). This is one of the most important points/questions of the manuscript to test but the experiments are done quite superficially. For example, why would one just take a single snapshot of one timepoint after transfection rather than a time course? How do they know the mutant is not more stable or expressed at higher levels than the wt and that is why it labels faster? This experiment must be done more thoroughly and be somehow related to the formation of ROs. They should look at what happens to zippered ER structures by EM or to the formation of ROs with the deletion mutant?

I do not see what the LD figure adds to the story. It does not make a strong point and could be

removed without further development.

Minor comments:
1. The figures have too many panels. It will help the readability and paper's flow to separate the figures into smaller ones.
2. Figure 2E. The NSP6 dynamics are stopped at 24s. Even if it is shown how the K22 increases mobility of NSP6, it would help to have data of longer dynamics for the control treatment.
3. Figure 2L. NSP6DSGF mutant induced the formation of the compartments 2h after transfection, what was the transfection time in the earlier figures with wild-type NSP6? Is the number and/or size of the compartments related to the transfection time and concentration?
4. Figure 2N. NSP6DSGF dimerizes more and is less mobile (shown by FLIP), but panel E shows that NSP6 is already immobile. This can be confusing, the FRAP experiments could be repeated with the mutant.

Referee #2 (Remarks to the Author):

The manuscript by Ricciardi and colleagues describe the the role of SARS-CoV-2 nsp6 in the context of the formation of replication organelles (RO). They first establish for SARS-CoV-2 nsp6 that it induces circular structures within the cytoplasm, similar as has been reported previously for IBV nsp6. By using IEM, they observed nsp6 at double-membraned lumen-less structures which they refer to as zippered ER. Nsp6 appears to undergo homodimerization, and the C-terminal region (aa 1-157) is sufficient to be recruited by full-length nsp6. Interestingly, the authors show that K22, a compound that has previously been shown to interfere with CoV ROs, and for which K22-resistance mapped to mutations in nsp6 (for HCoV-229E), also affects SARS-CoV-2 nsp6-induced membrane structures. The authors also assessed nsp6 containing the deltaSGF deletion that appeared in many SARS-CoV-2 variants during the pandemic, and for which functional data are not yet available. Based on a yet limited set of experiments the authors claim that deltaSGF-nsp6 has a higher proficiency in forming the nsp6 compartment. By including nsp3 and nsp4 in the analyses the authors demonstrate that RO-like structures generated by nsp3 and nsp4 are distinct with resect to localisation from the nsp6 compartment and that, by co-exression of nsp3/4 and nsp6, these compartments appear to interact and to be connected, but still show distinct ultrastructural localisation. Finally, the authors identify lipid droplets (LDs) to be in close proximity to ROs and that the LD-associated host factor DFCP1 interacts with nsp6 (but not with nsp3/4).

Overall, this is a very interesting and original study that is of significance for the field. In particular, the description of two distinct components of RO-like structures mediated my nsp3/4 and nsp6 is of great interest. However, the study will significantly become stronger if some of the analyses can be done under conditions of SARS-CoV-2 infection.

specific comments:

nsp6/K22: figure 2g shows nsp6 in proximity, but not exactly at dsRNA. While this section is

describing the effect of K22 on ROs, it would be interesting to see if this localisation pattern is also observed in K22-treated and SARS-CoV-2-infected cells. EM and/or immunoEM studies would be required to make the statement that membrane structures are impaired. Although the authors don't explicitly state this this would be a valuable addition to the study. EM studies are also needed to provide evidence for the "fewer circular structures" seen in K22 treated cells (line 29)

The section describing the detalSGF-nsp6 phenotype may benefit from additional experiments. For example, does K22 affect the nsp6 compartment differently if it is mediated by deltaSGF-nsp6? How do RO-like structures appear with nsp3/4 and deltaSGF-nsp6 co-expression?

The series of experiments shown in Figure 3 is very interesting. Is it possible to distinguish nsp3/4 and nsp6 localisation in virus-infected cells?

The section on LDs is leafing to the identification of DFCP1 and nsp6 interaction, and it would be important to perform analyses with DFCP1 knock-out (or knock-down) cells. Specifically, it would be interesting to assess SARS-CoV-2 replication in DFCP1 knock-out or nnbock-down cells.

Remarks for all figures:
* avoid blue, it's impossible to see
* annotate pannels more clearly (what are the conditions, what has been transfected, what has been stained and what is shown).
* insets are helpful to show a magnified reagion of interest. Sometimes the inset is not really a magnification and isn't helpful at all.
.

Referee #3 (Remarks to the Author):

In their submitted manuscript, Ricciardi et al. report that expression of SARS-CoV-2 NSP3-4 is sufficient to induce DMVs, similar to earlier reports for MERS-CoV and SARS-CoV (ref 4). Moreover, the authors show that expression of NSP6 triggers ER zippering, similar to what others have observed in SARS-CoV-2 infected cells. In addition to the membrane shaping function of NSP6, the authors present data that indicates NSP6 is involved in connecting viral replication structures to lipid droplets and speculate that this connection allows lipid transfer to support the formation of virus Replication Organelle Like Structure (ROLS). The authors present data that suggest these functions of NSP6 can be targeted to limit virus infection. Mutations in NSP6 are found in several of the currently circulating SARS-CoV-2 ‘variants of concern’ and the authors speculate that these mutations might provide a selective advantage by enhanced zippering of ER membranes. However, comparative analysis of viruses with and without these mutations (esp. the 106-108 deletion in NSP6) are not provided to compare the degree of ER zippering in an infection context and the possible advantage of virus replication exerted by this mutation.

Overall, the authors address an interesting aspect of the SARS-CoV-2 replication cycle. However, there are several major flaws in the current study that need to be addressed. Most importantly, the

data does not show a direct link between the NSP6 induced membrane zippers and DMV or viral RO biogenesis. Since a major claim of the manuscript is that NSP6 contributes to the biogenesis of the viral replication organelle, this function needs to be better defined. Additionally, the functional data in the manuscript is largely based on large halo like structures observed by fluorescence microscopy, but the underlying membrane structures are not clearly defined. These major points make it difficult to define the function of NSP6 and how this contributes to SARS-CoV-2 infection. Specific points below.

Major points

• The major failing of the current manuscript is in linking the function of NSP6 to a role in DMV formation or function. For the images shown, the structure of DMVs was similar in cells expressing NSP3/4 compared to cells expressing NSP3/4 and NSP6. Additionally, linker ER structures connected to DMVs are also visible in the NSP3/4 expressing cells without NSP6 (fig 3c and 3d). In order to make claims that NSP6 is involved in RO biogenesis and DMV growth, the authors need to quantifiably show a difference in RO formation in cells with or without NSP6. For instance, the authors could quantify the length and abundance of the ER linkers as well as the number and morphology of DMVs in the NSP3/4 expressing cells with and without NSP6. This analysis should also be done with the deltaSGF as well as with the K22.

• In the manuscript there is a large amount of heterogeneity between NSP6 induced structures observed by Fluorescence microscopy. In figure 1a NSP6 staining shows small cytosolic foci whereas in fig 1e, where the authors do functional assays, NSP6 staining shows large halo-like structures. These larger structures do not correlate with any of the membrane structures shown by EM. In order to make claims about these structures, the authors should use CLEM to define the underlying membrane morphologies.

• Although the immunofluorescence microscopy images are well quantified throughout the manuscript, there is a significant lack in image quantification for EM images. For instance, often do cells expressing NSP6 form long zippered ER membranes or circular zippered ER membrane structures?

• On line 12 of page 5 the authors suggest that the deltaSGF mutant has an increased membrane zippering capacity. However, this experiment is only done by Fluorescence microscopy. Increased zippered membranes should be shown quantitatively by EM. Also the authors should demonstrate equal protein levels between NSP6 and NSP6detla SGF expressing cells.

• Oligomerization assay need more proof, controls for IP (add one protein that is included in NSP6 structures and one that is not) and FRET. Put in the delta-Cterm which does not oligomerize.

• It is unclear from the manuscript what the K22 drug is doing to NSP6 structures and there is some inconsistency between figures. In figure 2e, there appears to be no difference in the NSP6 compartment by immunofluorescence. However, in figure 2f the authors show differences in NSP6 fluorescence structures when looking at cells that contain smaller NSP6 foci. This again highlights the heterogeneity in the morphology of NSP6 structures analyzed in different figures. To confirm that K22 is altering the NSP6 compartment, this should be shown by EM and/or CLEM to define the membrane structures that are represented by the fluorescence images.

• Extended data Figure 2g should include quantification to show that it is different between mutant and parental NSP6.

• In figure 3I the authors should show that there is no difference in the levels of protein expression between double or triple transfections. Is GFP alone added in double transfection? If not, this should

be included.
• In figure 4c, the authors us A92500 at a concentration of 20uM. The IC50 for this drug has been reported to be 7nM in vivo. Is the drug still specific at these concentrations? Is the drug cytotoxic to cells at these higher concentrations? These questions need to be addressed.
• Figure 4J: DFCP1 KD has been shown to increase LD numbers making it difficult to link the observed increase in LD number specifically to NSP6 (ref. PMID 31293035). Also, the effect of depletion should be shown in the context of virus infection.
• The function of NSP6 structures in allowing flow of lipids to the DMVs is not supported by the current data. The authors should show that there is a difference in lipid transfer to NSP3/4 puncta with or without NSP6 using FRAP experiments.

Minor
• Figure 1a: the total protein levels for each N or C tagged NSP6 should be shown.
• Figure 1d: untransfected cells should be shown for each marker.
• There is an inconsistency in the VAPA recruitment to NSP6 structures (Figure 1e vs 2b). In Figure 1e there is a strong re-localization of VAPA, but this is not the case in Figure 2b. This should be addressed
• How is “irregular” defined (Figure 2f). Describe the quantification.
• Figure 2g: The authors should quantify the proximity localization of NSP6 and dsRNA signal.
• Figure 2h: The authors should show additional cell viability assays to determine if the drug is affecting cells. LDH release shows cytopathic effect but does not determine cytostatic effects.
• Does K22 also limit function of the deltaSFG mutant NSP6?
• figure 3m: was this analysis done on cells that were confirmed to have all 3 proteins expressed?
• Figure 3g: The authors should quantify the frequency of the aggregates or single molecules on the DMVs or ER zippers
• figure 3I: the authors should show that there is no difference in the levels of protein expression between double or triple transfections. Is GFP alone added in double transfection? If not, this should be included.
• Figure 4b: quantification should be added
• Figure 4d: does transfection of the individual or combined viral proteins change LD numbers?

Author Rebuttals to Initial Comments:
Referee #1 (Remarks to the Author):

This manuscript investigates the role of the viral non-structural transmembrane proteins of SARS-CoV-2 (NSP6) in regulating the properties of the Nsp3/4-dependent replication organelle (RO) in tissue culture cells. This is an exciting question and timely subject. I think this story has great potential but some major points need to be addressed below.

We thank the reviewer for appreciating our work and for his/her constructive criticisms that we have addressed with new experimental data and with text clarifications.

Conclusions drawn from the data are that (N-term tagged) NSP6 drives formation of what appears to be a round NSP6 compartment by FM and a flat zippered ER cisternal compartment by immuno-EM. Both of which are near to NSP3/4 ROs. They show that the NSP6-dependent zippered ER membranes seen by EM are close to NSP3/4-dependent ROs and that exogenous expression of NSP6 will increase the abundance of these ROS. Thus there appears to be a link between NSP6 ER domains and NSP3/4 Ros even though they are non-overlapping. However, it baffles me why the flat zippered ER structures that NSP6 forms by EM are completely different in shape from the round structures imaged using FM. This needs to be resolved or explained. For example, an endosome has the same shape by FM that it does by EMT. Have the authors excluded whether the tagged NSP6 zippers some ER but the round structures seen by FM are NSP6 being degraded by lysosomes/endosomes?

We realized from the comments of the reviewers that we were not clear enough in describing the relationship between the NSP6 structures observed by IF and by EM. The gold standard method to study the correspondence between structures imaged by IF and their actual ultrastructure is correlative light electron microscopy (CLEM), identifying the ultrastructure of selected fluorescent objects. In the original manuscript we provided a CLEM analysis only for cells co-expressing the three membrane NSPs (NSP3/4/6). In the revised manuscript we have clarified this relationship at the very beginning of the manuscript by showing the CLEM data of cells expressing NSP6 alone. CLEM showed that the roundish or elongated NSP6 spots observed by IF corresponded respectively to the circular or linear zippered ER profiles (**Fig. 1e-g**), whose connection to the regular ER cisternae can be traced (**Fig. 1h**). For subsequent IF analysis we considered mainly circular NSP6 structures as a proxy for zippered ER membranes since linear structures were frequently closely associated with circular one (**Fig. 1h**) and, consequently, were difficult to resolve by regular confocal microscopy. We have clarified this in the text (page 3). We also would like to note that both linear and circular zippered NSP6 domains can be observed in association with NSP3/4 positive ROLs (see examples of such circular zippered structures in **Fig. 3d and Extended data Fig. 6h**). Interestingly, our EM analysis shows that zippered ER membranes may also assume a circular shape in SARS-CoV-2 infected cells (**Extended data Fig. 8f**).

In our initial search for compartments co-localizing with the round NSP6 structures we analyzed many different cellular compartments including endosomes (early and late), lysosomes and autophagosomes, but we could not find any co-localization (as shown only for autophagosomes in **Extended data Fig. 4h** of the original manuscript). In the revised manuscript we dedicate a panel to co-labeling images of NSP6 with endosomal, lysosomal and autophagosomal markers. The images

show that there is no colocalization of NSP6 with endolysosomes or autophagosomes (**Extended data Fig. 1d** and page 2).

By FM, NSP6 labeled compartments exclude luminal proteins but contain some membrane proteins. But what happened to the ER in these pictures? Why would ER proteins now only label blobs and no longer label the rest of the ER? I can't tell if these cells were just over transfected. This is also relevant to the FRAP analysis, the NSP6 compartments slowly recover membrane proteins and poorly recover "immobile" NSP6, but I'm not sure what these compartments are because the VAP labelled membranes are not normal ER anymore. Again, looks more like autophagy or a lysosome.

To show the extent of ER remodelling induced by NSP6 and to address the reviewer's concern, in the revised manuscript we have introduced images of the different ER markers when expressed alone (**Fig.1i**) in addition to the images showing NSP6 co-expressed with the same ER markers (**Fig.1j**). Comparing the two conditions it appears clearer than the soluble markers are not affected at all, whereas some membrane proteins partially enter the NSP6 compartment, while maintaining an extra-NSP6 pool. We believe the reviewer is referring to **Fig. 1e** of the original manuscript when he/she says" Why would ER proteins now only label blobs and no longer label the rest of the ER..." There we selected cells showing brighter and larger structures in view of the FRAP experiment to be performed and on acquisition planes that maximally highlight the roundish structures containing NSP6 and VAPA or Cb5. However, we realized that showing just the largest of the NSP6 structures at the expense of an overall view of the ER may be misleading since VAPA and Cb5 are still present on the general ER in addition to the roundish structures containing NSP6. We have introduced images in the revised manuscript that give a more precise idea of the overall distribution of VAPA and Cb5 in NSP6 expressing cells. A more precise assessment of the extent of ER remodelling in NSP6 expressing cells (assessed as the ratio between the NSP6-zippered and the regular ER) has been obtained from the morphometric ultrastructural analysis that shows that 59% of the ER is "regular ER" while 41% is zippered ER in NSP6 expressing cells (**Fig. 1d**).

As specified above, there is no co-localization between NSP6-labelled structures and lysosomal or autophagosomal markers (**Extended data Fig. 1d**).

Notably a 3 AA deletion (AA106-108) in NSP6 is found in four variants of concern. This leads to the interesting question of how does this deletion alter NSP6 behavior. They probe its solubility (fig 2m), its localization to NSP6 domains vs. general ER (fig 2o) and its ability to form NSP6 compartments (fig 2l). This is one of the most important points/questions of the manuscript to test but the experiments are done quite superficially. For example, why would one just take a single snapshot of one timepoint after transfection rather than a time course?

We thank the reviewer for his/her comment that prompted us to extend our comparative analysis of SGF-NSP6 with the reference NSP6. A major asset for this analysis was the development of stably transfected clones expressing either the reference or the SGF-NSP6 in an inducible manner. This allowed us to perform a complete time course (3, 5, 8 and 24 hrs) and quantitative analysis (number/size of the NSP6 structures and partitioning between ER and NSP6 compartment) of the expression of NSP6 in a relatively homogeneous cell population. With this analysis we could confirm

the initial observations in transiently transfected cells that the ΔSGF protein has a higher propensity to induce ER zippering. This was particularly evident at very early times of expression where ΔSGF-NSP6 induced ER-zippered structures while the reference NSP6, at the same time points and with similar levels of expression, was present in a diffuse pattern in the ER (**Fig. 2g, h**). A higher propensity of ΔSGF-NSP6 to zipper the ER was also evident over time with ΔSGF-NSP6 forming more numerous and larger structures and being more enriched in the NSP6 compartment compared to the reference NSP6 (**Fig. 2g, h**)**.** The results observed at the IF level were confirmed by IEM analysis which showed that ΔSGF-NSP6 is more concentrated on ER-zippered membranes compared to the reference NSP6 (**Fig. 2k**).

How do they know the mutant is not more stable or expressed at higher levels than the wt and that is why it labels faster? This experiment must be done more thoroughly and be somehow related to the formation of ROs.

We have addressed the questions raised by the reviewer and once again the inducible clones were a big help**. Extended data Fig. 5** shows that the reference and the SGF deletion mutant are expressed at comparable levels (**a**) while maintaining their different distribution pattern by IF analysis. It also shows that the reference and deletion mutant have a similar half-life as evaluated by pulse chase labelling (**b**). The only differences were a higher propensity of the mutant protein to homo-oligomerize, as indicated by more efficient self-association in co-IP assays(**d**), and its higher resistance to detergent extraction (**c**). As suggested by the reviewer (minor point 4), we have also compared the dynamics of ΔSGF-NSP6 with that of the reference NSP6 through FRAP experiments and found that the deletion mutant has an even lower mobility than the reference (**e, f**).

They should look at what happens to zippered ER structures by EM or to the formation of ROs with the deletion mutant?

In the original manuscript we provided EM images of the zippered ER induced by the deletion mutant. In the revised manuscript we performed morphometric analysis of the zippered ER induced by the reference and deletion mutant NSP6 and found that, similarly to the reference NSP6, the deletion mutant induced the zippering of the ER into linear and circular structures. However, we also found that the deletion mutant was more enriched on the zippered structures (**Fig. 2k**) and less abundant on regular ER, and induced zippering of larger ER surface (**Fig.2l**). This was likely due to the higher propensity of the deletion mutant to oligomerize. We have also performed a quantitative analysis in IF and EM of the ROLS formed in the presence of the reference and SGF deletion NSP6. We found that the deletion mutant, like the reference NSP6, is able to enhance the formation of NSP3/4 puncta and to organize them (**Fig. 3h**), but that the ROLS formed by the deletion mutant have more zippered connectors compared to the reference NSP6 (**Fig. 3n, Extended data Fig. 8a-c, Supplementary Movies 11, 12**). This correlated with an increase in the number of DMVs within ROLS of ΔSGF-expressing cells (**Extended data Fig. 8d**) indicating the higher capacity of the deletion mutant NSP6 to promote ROLS biogenesis.

The best demonstration of the relevance of our findings came from a comparative analysis of Calu-3 cells infected with the earlier lineages or the gamma variant of SARS-CoV-2 bearing the SGF deletion in NSP6. Although the gamma variant harbors additional mutations in other viral proteins (including

NSP3), making it difficult to dissect the contribution of any mutation to a particular phenotype, we did find a "connector phenotype" (i.e. more extensive zippered connector membranes in the RO of gamma-infected cells, **Fig. 3p-q, Extended data Fig. 8e-g**), which is fully consistent with our observation that the NSP6 deletion mutant has a higher ER zippering activity.

I do not see what the LD figure adds to the story. It does not make a strong point and could be removed without further development.

If on the one hand we agree with the reviewer that the "story" identifying NSP6 as a key factor in the biogenesis and organization of the RO would stand alone, we also believe that identifying a role for NSP6 in promoting the association of lipid droplets with the RO via DFCP1 adds a key piece to the puzzle of virus-host interactions and opens new avenues for future research. Importantly, in the revised manuscript we provide data indicating the DFCP1 is required for viral replication.

Minor comments:

1. **The figures have too many panels. It will help the readability and paper's flow to separate the figures into smaller ones.**

In principle we agree with the reviewer but the space limitations imposed by Nature guidelines for authors do not allow more than 4 main figures. To follow the reviewer's suggestion we have simplified the main figures by moving some panels to the supplementary figures.

2. Figure 2E. The NSP6 dynamics are stopped at 24s. Even if it is shown how the K22 increases mobility of NSP6, it would help to have data of longer dynamics for the control treatment.

Longer recovery dynamics (up to 400 sec) were already present in the graph in Fig. 2e of the original manuscript and in the Supplementary Movies 2-4. Following the reviewer's suggestion, we have now included images showing later time points (up to 60 secs) (**Extended data Fig. 4c**).

3. Figure 2L. NSP6DSGF mutant induced the formation of the compartments 2h after transfection, what was the transfection time in the earlier figures with wild-type NSP6? Is the number and/or size of the compartments related to the transfection time and concentration?

The transfection time in the earlier figures was 16 hours. However, in the revised manuscript, as specified above, we introduced a more detailed and time-resolved quantitative analysis of the NSP6 compartment in terms of number and size at the different times of expression taking advantage of the development of stably transfected inducible clones (**Fig. 2g, h**).

4. Figure 2N. NSP6DSGF dimerizes more and is less mobile (shown by FLIP), but panel E shows that NSP6 is already immobile. This can be confusing, the FRAP experiments could be repeated with the mutant.

As suggested by the reviewer, we have performed the FRAP experiments with the mutant (**Extended data Fig. 5g**). Even though, as the reviewer points out, the mobility of the reference NSP6 is already minimal (13% fluorescence recovery after 120 sec and 27% after 600 sec) that of the ΔSGF mutant is even lower (5% recovery after 120 sec and 15% recovery after 600 sec).

Referee #2 (Remarks to the Author):

The manuscript by Ricciardi and colleagues describe the role of SARS-CoV-2 nsp6 in the context of the formation of replication organelles (RO). They first establish for SARS-CoV-2 nsp6 that it induces circular structures within the cytoplasm, similar as has been reported previously for IBV nsp6. By using IEM, they observed nsp6 at double-membraned lumen-less structures which they refer to as zippered ER. Nsp6 appears to undergo homodimerization, and the C-terminal region (aa 1-157) is sufficient to be recruited by full-length nsp6. Interestingly, the authors show that K22, a compound that has previously been shown to interfere with CoV ROs, and for which K22-resistance mapped to mutations in nsp6 (for HCoV-229E), also affects SARS-CoV-2 nsp6-induced membrane structures. The authors also assessed nsp6 containing the ΔSGF deletion that appeared in many SARS-CoV-2 variants during the pandemic, and for which functional data are not yet available. Based on a yet limited set of experiments the authors claim that ΔSGF-nsp6 has a higher proficiency in forming the nsp6 compartment. By including nsp3 and nsp4 in the analyses the authors demonstrate that RO-like structures generated by nsp3 and nsp4 are distinct with respect to localisation from the nsp6 compartment and that, by co-expression of nsp3/4 and nsp6, these compartments appear to interact and to be connected, but still show distinct ultrastructural localisation. Finally, the authors identify lipid droplets (LDs) to be in close proximity to ROs and that the LD-associated host factor DFCP1 interacts with nsp6 (but not with nsp3/4).

Overall, this is a very interesting and original study that is of significance for the field. In particular, the description of two distinct components of RO-like structures mediated by nsp3/4 and nsp6 is of great interest. However, the study will significantly become stronger if some of the analyses can be done under conditions of SARS-CoV-2 infection.

We thank the reviewer for appreciating our work. We have followed his/her suggestion to perform some of the analyses in virus infected cells. In particular, by studying Calu-3 cells infected with SARS-CoV-2:

1. we confirmed our results with the recombinant NSPs by showing that the NSP6 compartment is close to but not overlapping that of NSP3 in cells infected with SARS-CoV-2;
2. we performed a comparative analysis of the replication organelle in Calu-3 cells infected with the earlier lineages or the gamma variant of SARS-CoV-2 bearing the 106-108 deletion. Although the gamma variant harbors additional mutations in other viral proteins (including NSP3), thereby demanding caution in ascribing their contribution to RO phenotypes, we found a “connector phenotype” attributable to NSP6 mutant. It manifested in more extensive zippered connector membranes in the RO of gamma-infected cells.

3. we found that DFCP1 is required for viral replication.

specific comments:

nsp6/K22: figure 2g shows nsp6 in proximity, but not exactly at dsRNA. While this section is describing the effect of K22 on ROs, it would be interesting to see if this localisation pattern is also observed in K22-treated and SARS-CoV-2-infected cells.

As suggested by the reviewer, we performed the experiments to visualize NSP6 in K22-treated cells infected with SARS-CoV-2. However, due to the inhibition of viral replication by K22, the NSP6 expression was consequently very much reduced precluding an analysis of its distribution (**Extended Data Fig. 7e**).

EM and/or immunoEM studies would be required to make the statement that membrane structures are impaired. Although the authors don't explicitly state this this would be a valuable addition to the study. EM studies are also needed to provide evidence for the "fewer circular structures" seen in K22 treated cells (line 29)

As suggested by the reviewer, we performed both standard EM and CLEM analysis of the NSP6 structures in cells treated with K22 and found that the irregular structures seen by IF correspond to extended zippered areas of the nuclear envelope (**Extended Data Fig. 4d-i**). Notably, EM data (our own and those deposited at EMPIAR 10490, a publicly available dataset containing electron-tomograms of SARS-CoV-2 infected Calu-3 cells https://www.ebi.ac.uk/empiar/EMPIAR-10490/) suggest that ROs/ROLs rarely form from the nuclear envelope. Thus, K22-induced redistribution of NSP6 to the nuclear envelope is expected to limit NSP6 potential to operate as a cue for ROs/ROLs biogenesis.

In addition, taking advantage of the stably transfected and inducible clones with a more homogeneous level of expression of NSP6, we could make a quantitative comparative analysis of untreated and K22 treated cells, and could show that K22 significantly and generally decreased the number of regular NSP6 structures (**Extended data Fig. 4a, b**) while inducing the formation of the aberrant elongated structures in 37% of cells.

The section describing the ΔSGF-nsp6 phenotype may benefit from additional experiments. For example, does K22 affect the nsp6 compartment differently if it is mediated by ΔSGF-nsp6?

How do RO-like structures appear with nsp3/4 and ΔSGF-nsp6 co-expression?

Following the referee's suggestion, we have performed a series of experiments to carry out a more extensive comparative analysis of the reference and ΔSGF-NSP6.

Firstly, we developed stably transfected cells expressing NSP6 reference and deletion forms in an inducible manner and performed a time resolved and quantitative analysis of the respective phenotypes (**Fig. 2g, h**).

Secondly, we analyzed the impact of K22 on ΔSGF-NSP6 and found that it inhibits the formation of the ΔSGF-NSP6 compartment, although to a slightly lower extent compared to the reference NSP6. Additionally, the mobility of ΔSGF was affected by K22 but to a lower extent compared to the reference NSP6 (**Extended data Fig. 5 f-h**).

Thirdly, we performed a quantitative IF and EM analysis of the ROLS formed in the presence of the reference and SGF deleted NSP6. We found that the deletion mutant, like the reference NSP6, is able to enhance and organize the formation of NSP3/4 puncta (**Fig. 3h**), but that the ROLS formed by the deletion mutant exhibit a more developed connector system and contained more DMVs compared to the reference NSP6 (**Fig. 3n, o, Extended data Fig.8 a-d, Supplementary Movies 11, 12**).

Finally, as mentioned above, we performed a comparative analysis of the replication organelle in Calu-3 cells infected with an early lineage or the gamma variant of SARS-CoV-2 bearing the 106-108 deletion and we found a "connector phenotype" (more extensive zippered connector membranes in the RO of gamma-infected cells; **Fig. 3p, q, Extended data Fig. 8 e-g, Supplementary Movies 13, 14**) attributable, with due caution, to the NSP6 deletion mutant.

The series of experiments shown in Figure 3 is very interesting. Is it possible to distinguish nsp3/4 and nsp6 localisation in virus-infected cells?

We thank the reviewer for this stimulating question that prompted us to look at the localization of NSPs in infected cells. Using commercially available antibodies against NSP6 and NSP3, which we further validated (**Extended Data Fig. 1c, 6c**), we could show that the NSP6 signal is close to but distinct from that of NSP3 in virus-infected cells (**Fig. 3b**), thus validating our observations with the recombinant viral proteins.

The section on LDs is leading to the identification of DFCP1 and nsp6 interaction, and it would be important to perform analyses with DFCP1 knock-out (or knock-down) cells. Specifically, it would be interesting to assess SARS-CoV-2 replication in DFCP1 knock-out or knock-down cells.

We have assessed the impact of DFCP1-KD on SARS-CoV-2 replication and found that the latter was inhibited by DFCP1 depletion (**Fig. 4l**).

Remarks for all figures:

*** avoid blue, it's impossible to see**

We have avoided the use of blue wherever possible

*** annotate pannels more clearly (what are the conditions, what has been transfected, what has been stained and what is shown).**

We have more clearly annotated the kind of treatment, transfection and staining in the panels.

*** insets are helpful to show a magnified reagion of interest. Sometimes the inset is not really a magnification and isn't helpful at all.**

For the sake of space and following the reviewer's suggestion, we have eliminated the insets where not needed.

Referee #3 (Remarks to the Author):

In their submitted manuscript, Ricciardi et al. report that expression of SARS-CoV-2 NSP3-4 is sufficient to induce DMVs, similar to earlier reports for MERS-CoV and SARS-CoV (ref 4). Moreover, the authors show that expression of NSP6 triggers ER zippering, similar to what others have observed in SARS-CoV-2 infected cells. In addition to the membrane shaping function of NSP6, the authors present data that indicates NSP6 is involved in connecting viral replication structures to lipid droplets and speculate that this connection allows lipid transfer to support the formation of virus Replication Organelle Like Structure (ROLS). The authors present data that suggest these functions of NSP6 can be targeted to limit virus infection. Mutations in NSP6 are found in several of the currently circulating SARS-CoV-2 'variants of concern' and the authors speculate that these mutations might provide a selective advantage by enhanced zippering of ER membranes.

However, comparative analysis of viruses with and without these mutations (esp. the 106-108 deletion in NSP6) are not provided to compare the degree of ER zippering in an infection context and the possible advantage of virus replication exerted by this mutation.

Prompted by the reviewer's comments we have performed a comparative analysis of Calu-3 cells infected with the early lineage or the gamma variant of SARS-CoV-2. The gamma variant, in addition to mutations in S and the 106-108 deletion in NSP6, harbors mutations in many other viral proteins (including NSP3), making it difficult to dissect the contribution of each mutant viral proteins to observed phenotypes and demanding caution in interpreting them. However, we did find a "connector phenotype" (i.e. more extensive zippered connector membranes in the RO of gamma variant-infected cells) that is fully consistent with our observation that the deletion mutant of NSP6 has a higher ER zippering activity (**Fig. 3n-q, Extended data Fig. 8e-g**).

We believe that establishing a correlation between the 106-108 deletion in NSP6 and a possible replication advantage of the variants is problematic, given the coexistence of multiple mutations in proteins that are also crucial for viral replication (e.g. NSP3, NSP13, ORF8).

We show here for the reviewer the comparative analysis of the gamma strain (with the SGF deletion) and early lineage (without) that we have performed in Calu-3 cells under conditions (binding at 4°C, i.e. adsorption, that allowed similar penetration level checked after 1h at 37°C) that reduce the impact of mutations in S, although, unfortunately, not that of mutations in the other viral proteins.

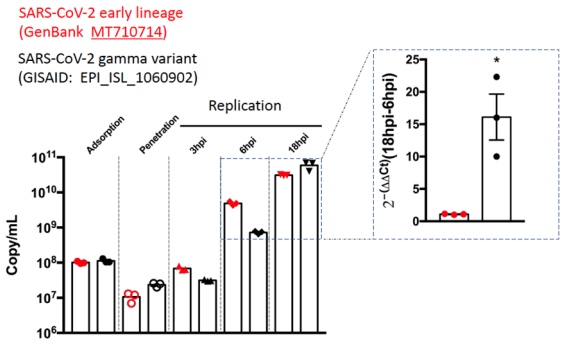

In agreement with reports on other SARS-CoV-2 lineages bearing the SGF deletion in NSP6 (Thorne, 10.1101/2021.06.06.446826), we observed that, after an initial lag, the SGF deletion strain achieved a higher replication rate between 6 and 18 hours (inset) after infection compared to the earlier isolate strain. Interestingly, this time window corresponds to the one that is accompanied by a marked increase in the size of DMVs in Calu-3 infected cells (Cortese et al. 2020). Thus, one might cautiously hypothesize that the SGF deletion could favor the growth of DMVs when needed. More speculatively, taking into consideration reports that the IFN response elicited in Calu-3 cells by SARS-CoV-2 (doi:10.1016/j.celrep.2020.108628) peaks at 12 hours and limits viral replication, that ΔSGF SARS-CoV-2 elicits a lower innate response in Calu-3 cells compared to the original strain (10.1101/2021.06.06.446826), and the tight relationship between innate response and UPR (https://doi.org/10.3390/ijms22115992), one could also hypothesize that the SGF deletion mutant with its more prominent zippering favors the formation of a “more protected” RO that is better isolated from UPR sensors and less active and/or slower in triggering innate response by the host cell.

Given the difficulty to assign these differences in replication to the different mutations present in gamma variant we have not introduced these data in the manuscript (referring to the existing literature). What we have instead reinforced in the revised manuscript, in order to gain more insights into the functional consequences of the SGF deletion, is the ultrastructural analysis of the reference and ΔSGF NSP6 expressed alone or in combination with NSP3/NSP4 (see below). As suggested by the reviewer, we have performed a quantitative morphometric analysis at IF and EM level.

Overall, the authors address an interesting aspect of the SARS-CoV-2 replication cycle. However, there are several major flaws in the current study that need to be addressed. Most importantly, the data does not show a direct link between the NSP6 induced membrane zippers and DMV or viral RO biogenesis. Since a major claim of the manuscript is that NSP6 contributes to the biogenesis of the viral replication organelle, this function needs to be better defined.

We thank the reviewer for this comment that prompted us to deepen our analysis of the functions of NSP6. In the original manuscript we identified NSP6 as a protein involved in the organization of the replication organelle of SARS-CoV-2 based on the observations that the NSP3-NSP4 positive structures (corresponding by CLEM to clusters of DMVs) were more numerous and more homogeneously distributed in the presence of NSP6 (**Fig. 3l, m,** original manuscript)**.** In revising the manuscript, and following the suggestion of the reviewer, we have extended our analysis of the role of NSP6 in RO biogenesis by performing comparative analysis by EM and EM tomography of DMVs induced by NSP3 and NSP4 in the presence or absence of NSP6, as detailed below.

Additionally, the functional data in the manuscript is largely based on large halo like structures observed by fluorescence microscopy, but the underlying membrane structures are not clearly defined.

We realized from the comments of the reviewers that we were not clear enough in describing the relationship between the NSP6 structures observed by IF and by EM. The gold standard method to study the correspondence between structures imaged by IF and their actual ultrastructure is correlative light electron microscopy (CLEM), identifying the ultrastructure of selected fluorescent objects. In the original manuscript we provided a CLEM analysis only for cells co-expressing the three membrane NSPs (NSP3/4/6). In the revised manuscript we have clarified this relationship at the very beginning of the manuscript by showing the CLEM data of cells expressing NSP6 alone. CLEM showed that the roundish or elongated NSP6 spots observed by IF corresponded respectively to the circular or linear zippered ER profiles (**Fig. 1e-g**), whose connection to the regular ER cisternae can be traced (**Fig. 1h**). For subsequent IF analysis we considered mainly circular NSP6 structures as a proxy for zippered ER membranes since linear structures were frequently closely associated with circular one (**Fig. 1h**) and, consequently, were difficult to resolve by regular confocal microscopy. We have clarified this in the text (page 3). We also would like to note that both linear and circular zippered NSP6 domains can be observed in association with NSP3/4 positive ROLs (see examples of such circular zippered structures in **Fig. 3d** and **Extended data Fig. 6h**).

These major points make it difficult to define the function of NSP6 and how this contributes to SARS-CoV-2 infection. Specific points below.

We thank the reviewer for appreciating our work and for raising constructive criticisms. We have addressed all the specific points raised by the reviewer with new experiments and with text clarifications as specified below.

Major points

• The major failing of the current manuscript is in linking the function of NSP6 to a role in DMV formation or function. For the images shown, the structure of DMVs was similar in cells expressing NSP3/4 compared to cells expressing NSP3/4 and NSP6. Additionally, linker ER structures connected to DMVs are also visible in the NSP3/4 expressing cells without NSP6 (fig 3c and 3d). In order to

make claims that NSP6 is involved in RO biogenesis and DMV growth, the authors need to quantifiably show a difference in RO formation in cells with or without NSP6. For instance, the authors could quantify the length and abundance of the ER linkers as well as the number and morphology of DMVs in the NSP3/4 expressing cells with and without NSP6. This analysis should also be done with the ΔSGF as well as with the K22.

We thank the reviewer for his/her comments that prompted us to perform a comparative morphometric analysis of the DMVs formed in the absence and presence of NSP6 (both reference and ΔSGF) leading to the discovery that NSP6 acts as an organizer of the DMV clusters.

We analyzed the DMVs in cells expressing NSP3/4 or NSP3/4/6 by EM and EM-tomography. We measured the size, number, shape and distribution of DMVs and analysed their connections with the regular ER.

We found that in the absence of NSP6, and as pointed out by the reviewer, DMVs can establish their own connections with the regular ER, but these connections are shorter, tubular in shape and have a larger diameter compared to those in cells co-expressing NSP6 where the connections have sheet-like geometry, higher length and almost completely zippered lumen (**Fig. 3l, m**). Importantly, while in the absence of NSP6 each DMV cluster had multiple connections with the ER (6 per cluster), with an average of only 3 DMVs per connection, the number of connections per DMV cluster was lower in the presence of NSP6 (2 per cluster) leading to higher number of vesicles (about 15) per connection (**Fig. 3m**).

These data indicate that NSP6 provides the DMVs with a common "zippered" communication channel with the ER. In the absence of NSP6 the DMVs establish independent connections with the ER which are tubular in shape and with a visible lumen. We envisage that the NSP6 connectors guarantee a more homogeneous feeding of lipids from the ER (while preventing the arrival of unwanted luminal ER proteins). It is tempting to speculate that the sheet-like geometry of the NSP6 connectors favours the arrival of selected lipids and thus affects the quality more than the quantity of lipids transferred from the ER to the DMVs. Consistent with this hypothesis, we found that the DMVs have a more homogeneous size (**Extended data Fig. 6d-f)** and a more regular circular shape in the presence of NSP6 than in its absence (**Fig. 3m**).

We also observed that the packing of the DMVs was higher in the presence of NSP6 as measured by DMV density (**Extended data Fig. 6g-i**), likely favouring homotypic interactions which are a prerequisite for the fusion of the external membrane and formation of vesicle packets in the later stages of infection.

Furthermore, following the reviewer's suggestion, we have also analysed by EM the ROLs (DMV clusters) in cells expressing the ΔSGF-NSP6 together with NSP3 and NSP4 and found that the system of zippered connectors was more developed with the ΔSGF-NSP6. This manifested in higher number of zippered linkers converging towards each individual DMV cluster and correlated with increase in the number of DMVs within ROLs (**Extended data Fig. 8a-d**). These findings suggest that expansion of zippered membranes in ROLs of ΔSGF-NSP6-expressing cells favours DMV biogenesis.

Finally, we have checked the effects of K22 in cells expressing NSP3/4 and NSP6 and found that while K22 had no effect on NSP3/4 puncta formation in cells expressing NSP3 and 4, it completely abolished

the ability of NSP6 to increase the number of the NSP3/4 puncta in cells expressing NSP3/4/6 (**Extended data Fig. 7a, b**).

• In the manuscript there is a large amount of heterogeneity between NSP6 induced structures observed by fluorescence microscopy. In figure 1a NSP6 staining shows small cytosolic foci whereas in fig 1e, where the authors do functional assays, NSP6 staining shows large halo-like structures. These larger structures do not correlate with any of the membrane structures shown by EM. In order to make claims about these structures, the authors should use CLEM to define the underlying membrane morphologies.

To address the reviewer's concerns on NSP6 structure heterogeneity, we developed stably transfected clones expressing NSP6 in an inducible manner. In this way we have achieved tighter control of the levels and times of expression as well as a general reduction in the heterogeneity of the NSP6 structures.

The reviewer rightly pointed out the difference in size between the NSP6 structures shown in Fig. 1e in comparison with those shown in other panels of the original manuscript. The difference is in part due to the selection of brighter and larger structures in the cells shown in Fig. 1e (in view of the FRAP experiment to be performed) and on the acquisition planes that highlight the roundish structures containing NSP6 and VAPA. However, we realized that showing only the largest NSP6 structures in living cells may be misleading so we provide images where FRAP analysis was performed on more representative and smaller circular structures (**Fig. 1k**, **l**).

As regards the correlation between the halo-like structures and the membrane morphology underlying these structures we realized that we were not clear enough in describing this correlation. In this context, we completely agree with the reviewer that the gold-standard method to study the correspondence between structures imaged by IF and their actual ultrastructure is correlative light electron microscopy (CLEM). In the revised manuscript we have clarified the relationship between the NSP6 halo-like structures seen in IF and the underlying membrane morphology by showing the CLEM data of cells expressing NSP6 as specified above in reply to the general comment.

• Although the immunofluorescence microscopy images are well quantified throughout the manuscript, there is a significant lack in image quantification for EM images. For instance, often do cells expressing NSP6 form long zippered ER membranes or circular zippered ER membrane structures?

Following the reviewer's suggestion, we have now quantified, wherever possible, the EM images of the different NSP6 structures in particular with regards to circular-linear morphology of zippered ER domains (**Fig. 1d**). By quantifying EM images of NSP6-expressing cells we found that about 41% of the ER surface area is occupied by zippered domains. We also noted that circular morphology of zippered membranes prevails over the linear (24% versus 17% of ER surface area).

• On line 12 of page 5 the authors suggest that the SGF mutant has an increased membrane zippering capacity. However, this experiment is only done by Fluorescence microscopy. Increased

zippered membranes should be shown quantitatively by EM. Also the authors should demonstrate equal protein levels between NSP6 and NSP6 SGF expressing cells.

Our conclusion that SGF NSP6 has an increased zippering activity stems from the observation, both at IF and EM level, that the deletion mutant is found more concentrated at the level of the NSP6 compartment in IF and zippered ER membranes (with a very low fraction localized in the general ER) as compared to the reference NSP6.

Following the reviewer's suggestion, we have now performed a quantitative comparative analysis of the two proteins at IF and EM level.

IF: A major asset in this direction came from the development of stably transfected clones expressing either the reference or the SGF NSP6 in an inducible manner. This allowed us to perform a complete time course (3, 5, 8 and 24 hrs) and quantitative (number/size of the NSP6 structures and partitioning between ER and NSP6 compartment) analysis of the expression of NSP6 in a homogeneous cell population. This analysis also takes in accounts CLEM data showing that well defined spots/foci of NSP6 signal in IF images correspond to zippered regions of the ER at the EM level (**Fig. 1e-h; Extended data Fig. 5i-k**).

With this analysis we could confirm our initial observations in transiently transfected cells that the SGF protein has a higher propensity to induce ER zippering. This was particularly evident at the very early times of expression where SGF was already capable of forming ER zippered structures while the reference NSP6, at the same time points and with similar levels of expression, was present in a diffuse pattern in the ER (**Fig. 2g, h**). A higher propensity of SGF NSP6 to zipper the ER was also evident throughout the time with SGF NSP6 forming more numerous and larger structures and being more enriched in the NSP6 compartment as compared to the reference NSP6 (**Fig. 2g, h**).

EM: We investigated whether SGF NSP6 expression leads to increase in ER zippering compared to WT-NSP6. This was a challenging task because as the Reviewer noted the expression levels of two NSP6 variants have to be taken in account. Therefore, we used immuno-EM images for quantification. This allowed us to assess both overall expression level of NSP6 (by quantifying NSP6-associated gold particles per cell) and ER surface occupied by zippered domains. Then surface area of zippered membranes was normalized for NSP6 expression level. This analysis revealed that the surface of zippered ER is higher in cells expressing deletion mutant (**Fig. 2l**).

We have also quantitively assessed the label density of the reference and SGF NSP6 on regular ER and zippered ER and found that the deletion mutant is more concentrated on the zippered ER regions (**Fig. 2k**) and hardly detectable on regular ER (**Fig. 2j**).

Finally, we quantified the levels of protein expression, both in terms of integrated intensity at IF level and by Western blot and pulse chase experiments and found that the two proteins, expressed at comparable levels (**Extended data Fig.5 a,b**), do exhibit difference in the extent of formation of the NSP6 compartment.

• Oligomerization assay need more proof, controls for IP (add one protein that is included in NSP6 structures and one that is not) and FRET. Put in the Cterm which does not oligomerize.

Following the reviewer's suggestions, we have repeated the IP and FRET experiments introducing one protein that is included in the NSP6 structures (ATL2) and one that is not (ERGIC53). Neither protein co-precipitated with NSP6 nor exhibited a significant FRET with NSP6, thus validating our IP and FRET approach to follow the oligomerization of NSP6 (**Extended data Fig. 3e**).

As regards the □C-terminal NSP6, it is unable to form the NSP6 compartment, however our recruitment assay in fluorescence suggests that it can oligomerize with the full length protein (**Fig. 2b**). We confirmed that this was the case both with co-IP and by FRET (**Fig. 2c** and **Extended data Fig. 3f**).

• It is unclear from the manuscript what the K22 drug is doing to NSP6 structures and there is some inconsistency between figures. In figure 2e, there appears to be no difference in the NSP6 compartment by immunofluorescence. However, in figure 2f the authors show differences in NSP6 fluorescence structures when looking at cells that contain smaller NSP6 foci. This again highlights the heterogeneity in the morphology of NSP6 structures analyzed in different figures. To confirm that K22 is altering the NSP6 compartment, this should be shown by EM and/or CLEM to define the membrane structures that are represented by the fluorescence images.

To address the reviewer comment concerning "the heterogeneity in the morphology of NSP6 structures" we set up stably transfected clones expressing NSP6 in an inducible manner. This system allowed us to monitor and quantify the impact of K22 on the formation of the NSP6 compartment in a more homogeneous cell population.

As shown in **Extended data Fig. 4**, we found that K22 (at 40 µM) induced a general decrease in the number of NSP6 structures (**Extended data Fig. 4 a, b**). When analyzed by FRAP the NSP6 structures contained a more mobile NSP6 protein pool relative to untreated cells.

In addition, in 37% of cells, K22 induced "irregular" NSP6 structures consisting of elongated perinuclear structures (**Extended data Fig. 4a, b**). CLEM analysis showed that these structures corresponded to areas of the nuclear envelope undergoing extensive zippering (**Extended data Fig. 4d**). The EM analysis confirmed the presence of large zippered areas in the nuclear envelope (**Extended data Fig. 4e, f, h**).

Although the reasons for this relocation of NSP6 towards the NE remain to be investigated, it is important to underscore that NE represents a bad substrate for RO biogenesis. Our own EM and tomography data suggest that DMVs or their clusters never form from the NE. Along the same lines, the tomography data series of SARS-CoV-2 infected Calu-3 cells deposited in EMPIAR 10490, a publicly available dataset containing electron-tomograms of SARS-CoV-2 infected Calu-3 cells (https://www.ebi.ac.uk/empiar/EMPIAR-10490/) indicate that the NE appears to be an unfavourable area for the formation of DMVs. These data show that the DMVs very rarely originate from the NE (only 5 DMVs annotated as "DMV in nuclear envelope" in approximately three thousand DMVs analyzed) compared to the regular ER. Thus, we can speculate that the impaired formation of the NSP6 compartment and the shift of NSP6 zippering activity towards the nuclear envelope might contribute to the inhibition of SARS-CoV-2 replication observed with K22.

• Extended data Figure 2g should include quantification to show that it is different between mutant and parental NSP6.

We have performed this quantification (**Fig. 2k**) that confirmed that association of mutant NSP6 on zippered ER is higher than that of parental NSP6.

• In figure 3I the authors should show that there is no difference in the levels of protein expression between double or triple transfections. Is GFP alone added in double transfection? If not, this should be included.

We followed the suggestion of the reviewer and found that the co-expression of NSP6 or of GFP alone does not significantly affect the levels of NSP3/NSP4 (**Extended data Fig. 6a**).

• In figure 4c, the authors us A92500 at a concentration of 20uM. The IC50 for this drug has been reported to be 7nM in vivo. Is the drug still specific at these concentrations? Is the drug cytotoxic to cells at these higher concentrations? These questions need to be addressed

The concentrations used in the study were based on previously reported effects of DGAT inhibitor on HCV and SARS-CoV-2 infection (Herker et al., 2010; Dias et al., 2020). No cytotoxic effect was observed at the concentrations used, as evaluated by LDH assay or crystal violet (see below). Treatment with A922500 inhibited the LD formation triggered by SARS-CoV-2 infection in A549 human epithelial cells and in primary human monocytes in a dose dependent manner, with 50% effective concentration value of 0.108 µM for A549 cells and 0.711 µM for human monocytes (Dias et al., 2020). In this study, we observed a dose dependent effect of A922500 with an EC_{50} of 13 µM for LDs and 9 µM for viral replication in Calu-3 cells infected with SARS-CoV-2. At higher concentrations A922500 has been reported to inhibit DGAT2 in addition to the effect on DGAT1. However, a major effect of A922500 on DGAT1 in our system is supported by the similar effect of DGAT1 knockdown by siRNA on SARS-CoV-2 replication inhibition.

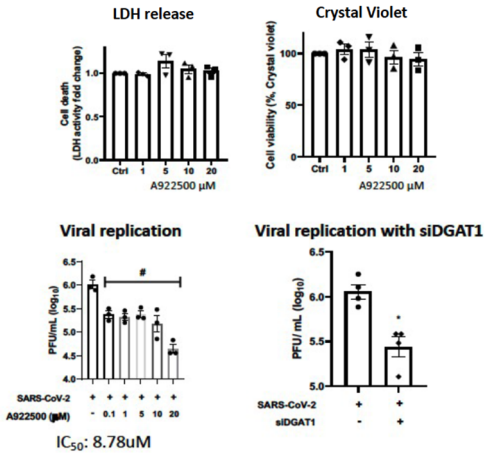

Figure 4J: DFCP1 KD has been shown to increase LD number making it difficult to link the observed increase in LD number specifically to NSP6 (ref. PMID 31293035). Also, the effect of depletion should be shown in the context of virus infection.

To address the reviewer's concerns and to further dissect the role of NSP6 in the decrease of LD consumption in DFCP1-depleted cells, we have quantified the LDs in cells expressing NSP3 and NSP4 or NSP3/4/6 in mock or DFCP1-depleted cells. The comparison confirmed that the presence of NSP6 induces a higher consumption of LDs in mock-treated cells and magnified the inhibitory effect of DFCP1 depletion on LD consumption. Indeed, even though the depletion of DFCP1, as rightly pointed out by the reviewer, decreases the consumption of LDs in the absence of NSP6 (with a 40% increase of LD area), it was much more effective in reducing the consumption in NSP6-expressing cells (with an 80% increase of LD area). In fact, the gap between NSP3/4 expressing cells and NSP3/4/6 expressing cells in terms of LD consumption is decreased upon DFCP1 depletion (**Fig. 4j**).

Finally, we have assessed the impact of DFCP1 in the context of virus infection in Calu-3 cells and found that SARS-CoV-2 replication is impaired by DFCP1 depletion (**Fig. 4l).**

We have also looked at the LDs in infected cells under mock conditions or upon depletion of DFCP1. As reported for other cell lines, SARS-CoV-2 infection increases the LDs in Calu-3 cells. DFCP1-depletion inhibited viral replication and thus prevented the virus-induced increase of LDs. We show below the data for the reviewer.

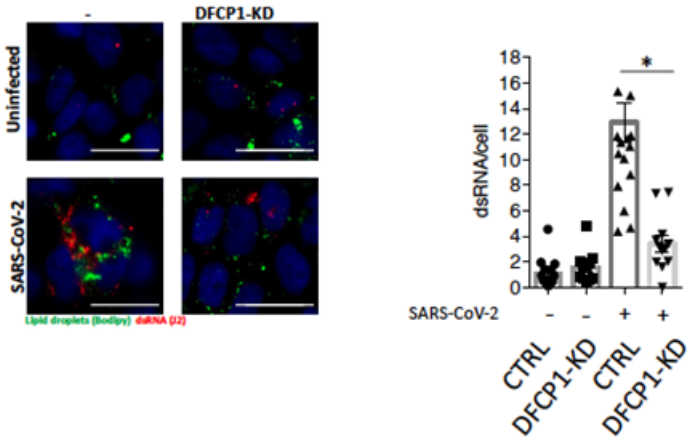

• The function of NSP6 structures in allowing flow of lipids to the DMVs is not supported by the current data. The authors should show that there is a difference in lipid transfer to NSP3/4 puncta with or without NSP6 using FRAP experiments.

To address the reviewer's question about the difference in lipid transfer to NSP3/4 puncta with or without NSP6 we monitored the transfer of LD-derived lipids to the NSP3/4 puncta. We exploited the protocol described in Rambold et. al (Developmental Cell 32, 678–692, 2015) designed to follow the

destiny of lipids mobilized from LD. Applying this protocol, based on the loading and wash out of BODIPY 558/568 C12 (a saturated fatty acid analog), we found that the presence of NSP6 allows a more efficient transfer of BODIPY 558/568 C12 to the NSP3/4 puncta (**Extended data Fig. 10e**).

Minor

• Figure 1a: the total protein levels for each N or C tagged NSP6 should be shown.

We have checked the level of expression of N- and C-tagged NSP6 both by measuring the integrated fluorescence intensity in IF and by WB. We confirmed that cells expressing N- and C-tagged NSP6 at the same levels (**Extended data Fig. 1b**) are distributed differently, with a distinct NSP6 compartment or a diffuse ER distribution, respectively.

• Figure 1d: untransfected cells should be shown for each marker.

In the revised manuscript we show each marker in untransfected cells (**Fig. 1i**).

• There is an inconsistency in the VAPA recruitment to NSP6 structures (Figure 1e vs 2b). In Figure 1e there is a strong re-localization of VAPA, but this is not the case in Figure 2b. This should be addressed

The difference is due in part to the fact that in Fig. 1e VAPA is exogenously expressed as GFP-VAPA while in Fig. 2b it is the endogenous protein detected with an antibody, and in part, as mentioned above, to the fact that in Fig. 1e cells with brighter and larger structures were chosen in view of the FRAP experiment to be performed and on acquisition planes that highlight the roundish structures containing NSP6 and VAPA. However, we realized that showing just the largest of the NSP6 structures in living cells may be misleading so we provide images where FRAP analysis was performed also on more representative and smaller circular structures (**Fig. 1k**).

• How is "irregular" defined (Figure 2f). Describe the quantification.

We now define what we mean by irregular structures: these are elongated structures in the perinuclear area. More importantly, we provide EM analysis of these structures by CLEM and EM (**Extended data Fig. 4 d-i**) and also report a quantitative assessment of the effects of K22 on the NSP6 compartment. For the quantitative analysis (**Extended Fig. 4a** and Methods) we took advantage of the development of stably transfected clone expressing NSP6 in inducible manner that allowed the analysis of a more homogeneous cell population**.**

• Figure 2g: The authors should quantify the proximity localization of NSP6 and dsRNA signal. We have quantified the proximity of NSP6 and dsRNA signal which is shown in **Extended data Fig. 7e.**

• Figure 2h: The authors should show additional cell viability assays to determine if the drug is affecting cells. LDH release shows cytopathic effect but does not determine cytostatic effects.

Cell number and cell viability after treatment with either K22 or A922500 were assessed by crystal violet staining, cell morphology analysis, or LDH assay. No cytostatic or cytotoxic effect of the drugs was observed at the concentrations used. We have introduced this clarification in the manuscript (see Methods).

• Does K22 also limit function of the SFG mutant NSP6?

We have performed the experiment and found that K22 was active on SGF NSP6, albeit with a slightly lower efficiency than on the reference NSP6.

• figure 3m: was this analysis done on cells that were confirmed to have all 3 proteins expressed?

Yes, we cross checked the presence of the three proteins each possessing a different tag.

• Figure 3g: The authors should quantify the frequency of the aggregates or single molecules on the DMVs or ER zippers.

We believe that we did not provide a clear enough explanation for this figure. Gold labelling in this figure (**Fig. 3e** in revised manuscript) does not correspond to single molecules or aggregates of the same protein. Therefore, their quantification cannot be used to judge regarding monomeric or oligomeric protein fractions.

Small gold particles represent NSP6, while large gold clusters represent NSP3. This double immune-EM labelling was done using secondary antibodies conjugated to ultra-small gold particles, which were enhanced for shorter period (to have small particles for NSP6) and longer period (to have large particles for NSP3). It is known that longer enhancement time causes the formation of larger gold particles (clusters) with an irregular shape. This frequently leads to confusion and interpretation of these large particles/clusters as a sign of oligomerization-aggregation of single protein molecules. We have explained this and the procedure in Methods, and indicated “see Methods” in the figure legend.

• figure 3I: the authors should show that there is no difference in the levels of protein expression between double or triple transfections. Is GFP alone added in double transfection? If not, this should be included.

We have performed these control experiments introducing a GFP in the double transfection and found that it did not impact the levels of NSP3/NSP4 (**Extended data Fig.6a**).

• Figure 4b: quantification should be added?

We have quantified the proximity between dsRNA or NSP6 and LDs (**Fig. 4b**).

• Figure 4d: does transfection of the individual or combined viral proteins change LD numbers?

As specified above, we have measured the LD area in NSP3/4 transfected cells and in NSP3/4/6 transfected cells and found that the presence of NSP6 (but not of NSP3 or 4) induces a consumption of LDs (**Fig 4j**).

Reviewer Reports on the First Revision:

Referees' comments:

Referee #1 (Remarks to the Author):

The goal of this paper was to investigate the role of SARS-CoV-2 protein NSP6 in regulating the biogenesis of the viral replication organelle (RO) induced in cells expressing the CoV-2 structural proteins NSP3/4.

A major conclusion of the paper was to describe two structural domains that are induced by NSP6. Their CLEM data shows that two interconnected structural compartments are induced upon NSP6 or mutant NSP6 expression: NSP6-labelled round compartments and to a lesser extent a zippered ER compartment. The authors now show in a time course the relative speed at which NSP6 deletion mutant vs wt NSP6 to form the round compartments. Although the NSP6 mutant forms NSP6 round compartments faster, it remains unknown whether these NSP6 compartments are a critical path precursor to ROs, an off-target rearrangement of ER membranes, or some sort of ER-associated degradative compartment, which remains a shortcoming of the story because it limits the significance of describing this domain.

A second conclusion of the paper is that co-expression of NSP6 even if not exactly co-localized can organize and/or promote formation of NSP3/NSP4 ROs. This does appear to be true, but by what mechanism is not shown.

I still do not agree with the third conclusion of this paper, which is why I suggested it be removed. The data in Fig 4 is not compelling enough to suggest a structural or functional interaction between LDs and NSP6 domains or ROs. The 3 vesicle populations are near each other, but do not appear to overlap, and because all 3 structures are very dense in the ROIs analyzed I suspect the same level of co-localization would be seen in merged images where one of the channels was randomly rotated.

In a related note, I understand that DFCP1 is being proposed as some relevant LD-ER tether required here for RO biogenesis, but two issues concern me about this conclusion. First, why is the GFP-DFCP1 construct not localized to the ER in the first control panel of Fig 4f, if it is an ER membrane protein? This makes it seem like there something wrong with this expression construct? Second, the data showing that GFP-DFCP1 co-localizes upon NSP6 expression around NSP6 vesicles does not show a tethering interaction. The trend I see throughout the figures is that NSP6 expression causes ER membranes to wrap around NSP6 vesicular domains (by FM and EM) and for example see snapshots for: GFP-DFCP1, Atl2, Rab18, KDELR, VAP and even BODIPY PC.

Other minor comments:
- In the rebuttal, the authors say that circular NSP6 domains by FM are taken as proxy throughout the rest of the paper for zippered ER- this is unreasonable as they are clearly two very different kinds of compartments by EM.

Referee #2 (Remarks to the Author):

The revised manuscript appears greatly improved and the authors have responded appropriately to my comments. In particular it is acknowledged that there's now at several locations cross reference to data with SARS-CoV-2 infection. The manuscript is very data rich, but well written so that readers are nicely guided through the complex matter. Many details, that probably would deserve entire independent studies, are included in this work, and collectively, this study significantly extends our knowledge on CoV ROs, and the pivotal role that nsp6 has to play.

Referee #3 (Remarks to the Author):

>In their revised manuscript, Ricciardi et al. have addressed the points raised by this reviewer by performing additional experiments and quantifying the previously shown qualitative data. The authors have introduced some new tools (e.g., inducible NSP6 expression) to support their previously shown findings and extensively quantified the data shown in the earlier version of their manuscript. These additions have significantly improve the manuscript.

However, there are still few points that need to be addressed via clarification, reanalysis, and new experimentation. In short, there were several quantifications added to better describe the role of NSP6 towards DMV biogenesis. These overall are convincing to suggest the role NSP6 in DMV biogenesis. However, some of these measurements either do not always correlate between the early-lineage NSP6 and the ΔSGF-NSP6 as compared to the DMVs formed in their absence, or they need a separate quantification feature. For example, since the authors define the same ER connectors with the DMVs in the absence or presence of NSP6, the highly zippered ER seen in the ΔSGF-NSP6 may require a new quantification.

In addition, the effect of K22 on DMV biogenesis via its effect on NSP6 is still not sufficiently clarified. The mock control showing the effect of K22 on cells in the absence of NSP6 expression is missing, and the strong effect of K22 on NSP6 relocalisation is not shown for its effect on DMV biogenesis by measuring DMV numbers and morphology.

More detailed replies are given below to those authors' responses, where I still have comments.<

Referee #3 (Remarks to the Author):

Overall, the authors address an interesting aspect of the SARS-CoV-2 replication cycle. However, there are several major flaws in the current study that need to be addressed. Most importantly, the

data does not show a direct link between the NSP6 induced membrane zippers and DMV or viral RO biogenesis. Since a major claim of the manuscript is that NSP6 contributes to the biogenesis of the viral replication organelle, this function needs to be better defined.
We thank the reviewer for this comment that prompted us to deepen our analysis of the functions of NSP6. In the original manuscript we identified NSP6 as a protein involved in the organization of the replication organelle of SARS-CoV-2 based on the observations that the NSP3-NSP4 positive structures (corresponding by CLEM to clusters of DMVs) were more numerous and more homogeneously distributed in the presence of NSP6 (Fig. 3l, m, original manuscript). In revising the manuscript, and following the suggestion of the reviewer, we have extended our analysis of the role of NSP6 in RO biogenesis by performing comparative analysis by EM and EM tomography of DMVs induced by NSP3 and NSP4 in the presence or absence of NSP6, as detailed below.

>The extensive quantifications done by the authors for this part is commendable. The authors have added several quantification measures that are presented mostly in Fig. 3l, m. These quantifications overall imply that DMVs formed in the absence of NSP6 are more connected to the ER and are not homogenous in shape. The expression of NSP6 reduces the number of ER connections which correlates with the formation of more DMVs per connection. Whereas this correlation is shown to work well with the NSP6 from the early lineage SARS-CoV-2, the ΔSGF-NSP6 showed more DMVs per cluster, yet showed more ER connectors per DMV cluster, indicating that reducing the ER connections (or zippered connectors) to the DMV cluster may not be the only NSP6 function that leads to more DMVs per cluster. This is also in contrast to the suggestion from the authors that the expansion of the zippered membranes may favor DMV biogenesis. One possibility could stem from the fact that ER connectors that are quantified in Fig. 3m (from early lineage SARS-CoV-2) are different from the zippered connectors shown for ΔSGF-NSP6, which has to be either quantified differently or should be acknowledged.<

Major points
• The major failing of the current manuscript is in linking the function of NSP6 to a role in DMV formation or function. For the images shown, the structure of DMVs was similar in cells expressing NSP3/4 compared to cells expressing NSP3/4 and NSP6. Additionally, linker ER structures connected to DMVs are also visible in the NSP3/4 expressing cells without NSP6 (fig 3c and 3d). In order to make claims that NSP6 is involved in RO biogenesis and DMV growth, the authors need to quantifiably show a difference in RO formation in cells with or without NSP6. For instance, the authors could quantify the length and abundance of the ER linkers as well as the number and morphology of DMVs in the NSP3/4 expressing cells with and without NSP6. This analysis should also be done with the ΔSGF as well as with the K22.
We thank the reviewer for his/her comments that prompted us to perform a comparative morphometric analysis of the DMVs formed in the absence and presence of NSP6 (both reference and ΔSGF) leading to the discovery that NSP6 acts as an organizer of the DMV clusters.
We analyzed the DMVs in cells expressing NSP3/4 or NSP3/4/6 by EM and EM-tomography. We measured the size, number, shape and distribution of DMVs and analysed their connections with the regular ER.
We found that in the absence of NSP6, and as pointed out by the reviewer, DMVs can establish their

own connections with the regular ER, but these connections are shorter, tubular in shape and have a larger diameter compared to those in cells co-expressing NSP6 where the connections have sheet-like geometry, higher length and almost completely zippered lumen (Fig. 3l, m). Importantly, while in the absence of NSP6 each DMV cluster had multiple connections with the ER (6 per cluster), with an average of only 3 DMVs per connection, the number of connections per DMV cluster was lower in the presence of NSP6 (2 per cluster) leading to higher number of vesicles (about 15) per connection (Fig. 3m).
These data indicate that NSP6 provides the DMVs with a common "zippered" communication channel with the ER. In the absence of NSP6 the DMVs establish independent connections with the ER which are tubular in shape and with a visible lumen. We envisage that the NSP6 connectors guarantee a more homogeneous feeding of lipids from the ER (while preventing the arrival of unwanted luminal ER proteins). It is tempting to speculate that the sheet-like geometry of the NSP6 connectors favours the arrival of selected lipids and thus affects the quality more than the quantity of lipids transferred from the ER to the DMVs. Consistent with this hypothesis, we found that the DMVs have a more homogeneous size (Extended data Fig. 6d-f) and a more regular circular shape in the presence of NSP6 than in its absence (Fig. 3m).
We also observed that the packing of the DMVs was higher in the presence of NSP6 as measured by DMV density (Extended data Fig. 6g-i), likely favouring homotypic interactions which are a prerequisite for the fusion of the external membrane and formation of vesicle packets in the later stages of infection.
Furthermore, following the reviewer's suggestion, we have also analysed by EM the ROLs (DMV clusters) in cells expressing the ΔSGF-NSP6 together with NSP3 and NSP4 and found that the system of zippered connectors was more developed with the ΔSGF-NSP6. This manifested in higher number of zippered linkers converging towards each individual DMV cluster and correlated with increase in the number of DMVs within ROLs (Extended data Fig. 8a-d). These findings suggest that expansion of zippered membranes in ROLs of ΔSGF-NSP6-expressing cells favours DMV biogenesis.
Finally, we have checked the effects of K22 in cells expressing NSP3/4 and NSP6 and found that while K22 had no effect on NSP3/4 puncta formation in cells expressing NSP3 and 4, it completely abolished the ability of NSP6 to increase the number of the NSP3/4 puncta in cells expressing NSP3/4/6 (Extended data Fig. 7a, b).

>The authors have made substantial efforts to describe the qualitative differences observed in DMVs in the presence or absence of NSP6 into quantitative measurements. Particularly interesting is the increase in the number of DMVs seen in the clusters in the presence of NSP6 and ΔSGF-NSP6. These additional data have improved the manuscript and better describe the effect of NSP6 on DMV biogenesis.

However, there are some details that need attention. As described in the comment above, some quantified features do not always fully correlate with the function of NSP6 towards increasing the number of DMVs in the cluster or inducing homogenous size, e.g., the number of ER connectors. This is either due to the lack of some measurements (e.g., DMV diameter in the ΔSGF-NSP6) or using the same measurement for the ER connectors in presence or absence of NSP6. This should be clarified or acknowledged better. The authors should also comment if the diameters of DMVs uniformly decrease to compensate the increase in its number as seen with early lineage NSP6 (Extended data

Fig. 6f), by including this data for the ΔSGF-NSP6. If so, the increased “DMV expansion” might not be related to the role of NSP6 in DMV biogenesis.

In addition, the authors showed that K22 causes a change in the localization of NSP6, but the impact of K22 on DMV biogenesis (number and morphology) is missing. This data is desirable to fully understand the contribution of NSP6 towards DMV biogenesis, given the strong impact of K22 on NSP6 localisation.<

• Oligomerization assay need more proof, controls for IP (add one protein that is included in NSP6 structures and one that is not) and FRET. Put in the ∆–Cterm which does not oligomerize.
Following the reviewer’s suggestions, we have repeated the IP and FRET experiments introducing one protein that is included in the NSP6 structures (ATL2) and one that is not (ERGIC53). Neither protein co-precipitated with NSP6 nor exhibited a significant FRET with NSP6, thus validating our IP and FRET approach to follow the oligomerization of NSP6 (Extended data Fig. 3e).
As regards the ∆C-terminal NSP6, it is unable to form the NSP6 compartment, however our recruitment assay in fluorescence suggests that it can oligomerize with the full length protein (Fig. 2b). We confirmed that this was the case both with co-IP and by FRET (Fig. 2c and Extended data Fig. 3f).

>These results suggest that the dimer and oligomer formation between NSP6 molecules can still occur in the absence of the C-terminal region of NSP6 that harbors the amphipathic helix. This should be reflected in the model (Extended Fig 11) where NSP6 dimers are linked via the C-terminal residues.<

• It is unclear from the manuscript what the K22 drug is doing to NSP6 structures and there is some inconsistency between figures. In figure 2e, there appears to be no difference in the NSP6 compartment by immunofluorescence. However, in figure 2f the authors show differences in NSP6 fluorescence structures when looking at cells that contain smaller NSP6 foci. This again highlights the heterogeneity in the morphology of NSP6 structures analyzed in different figures. To confirm that K22 is altering the NSP6 compartment, this should be shown by EM and/or CLEM to define the membrane structures that are represented by the fluorescence images.
To address the reviewer comment concerning “the heterogeneity in the morphology of NSP6 structures” we set up stably transfected clones expressing NSP6 in an inducible manner. This system allowed us to monitor and quantify the impact of K22 on the formation of the NSP6 compartment in a more homogeneous cell population.
As shown in Extended data Fig. 4, we found that K22 (at 40 μM) induced a general decrease in the number of NSP6 structures (Extended data Fig. 4 a, b). When analyzed by FRAP the NSP6 structures contained a more mobile NSP6 protein pool relative to untreated cells.
In addition, in 37% of cells, K22 induced “irregular” NSP6 structures consisting of elongated perinuclear structures (Extended data Fig. 4a, b). CLEM analysis showed that these structures corresponded to areas of the nuclear envelope undergoing extensive zippering (Extended data Fig. 4d). The EM analysis confirmed the presence of large zippered areas in the nuclear envelope

(Extended data Fig. 4e, f, h).
Although the reasons for this relocation of NSP6 towards the NE remain to be investigated, it is important to underscore that NE represents a bad substrate for RO biogenesis. Our own EM and tomography data suggest that DMVs or their clusters never form from the NE. Along the same lines, the tomography data series of SARS-CoV-2 infected Calu-3 cells deposited in EMPIAR 10490, a publicly available dataset containing electron-tomograms of SARS-CoV-2 infected Calu-3 cells (https://www.ebi.ac.uk/empiar/EMPIAR-10490/) indicate that the NE appears to be an unfavourable area for the formation of DMVs. These data show that the DMVs very rarely originate from the NE (only 5 DMVs annotated as "DMV in nuclear envelope" in approximately three thousand DMVs analyzed) compared to the regular ER. Thus, we can speculate that the impaired formation of the NSP6 compartment and the shift of NSP6 zippering activity towards the nuclear envelope might contribute to the inhibition of SARS-CoV-2 replication observed with K22.

>Though the results depicting the change in localization of NSP6 puncta close to the nuclear envelope is shown clearly, the suggestion that this led to the zippering of the nuclear envelope is rather premature. The images (Extended data Fig. 4 f-h) showing the described zippering of the nuclear envelope are not clear enough to make this claim. This should be supported further using an ER membrane marker that associates with NSP6 using immunofluorescence staining (Fig. 1j, Extended data Fig. 2).

In addition, the mock control for the effect of K22 on cells in the absence of NSP6 expression is missing. This is important to rule out the possibility that K22 alone can induce changes to the ER membranes close to the nuclear envelope or nuclear envelope itself.<

• Figure 4d: does transfection of the individual or combined viral proteins change LD numbers?
As specified above, we have measured the LD area in NSP3/4 transfected cells and in NSP3/4/6 transfected cells and found that the presence of NSP6 (but not of NSP3 or 4) induces a consumption of LDs (Fig 4j).
O
>In the final model, NSP6 dimers appear to interact via N-term to C-term, which is contrary to the data shown in the revised manuscript where NSP6 dimers still interacted in the absence of the loss of C-term residues harboring the amphipathic helix. The authors should harmonise their model accordingly.<

Author Rebuttals to First Revision:

Referees' comments:

Referee #1 (Remarks to the Author):

The goal of this paper was to investigate the role of SARS-CoV-2 protein NSP6 in regulating the biogenesis of the viral replication organelle (RO) induced in cells expressing the CoV-2 structural proteins NSP3/4. A major conclusion of the paper was to describe two structural domains that are induced by NSP6.
A major conclusion of our paper is that NSP6 and NSP3/4 form two distinct domains of the replication organelle (RO): the connectors made of zippered ER and the DMVs, respectively.

Their CLEM data shows that two interconnected structural compartments are induced upon NSP6 or mutant NSP6 expression: NSP6-labelled round compartments and to a lesser extent a zippered ER compartment.
The reviewer appears to consider the "*NSP6-labelled round compartment*" as having a different membrane nature than the zippered ER. Our EM, IEM and electron tomography analyses show that both round and linear NSP6 compartments consist of zippered ER membranes (Fig.1 b-d, Extended data Fig. 1f, g). The zoomed area (220.000X) in Extended data Fig. 1g (of the previous version, 1i of the present one) most clearly shows that both circular and linear structures are made of zippered ER (i.e. two membrane layers without lumen).
From the reviewer's comment we realize that this was probably not equally clear for the IEM images (Fig. 1b). We have therefore provided higher enlargements (135.000X and 220.000X) also for the immuno-EM analysis in the revised manuscript (Extended data Fig.1f,g), which clearly show that the *NSP6-labelled round compartment* is made of circular zippered ER membranes.
We also provide additional images below (**Figure 1**) for the reviewer showing that the circular NSP6-positive structures are lined by two-membranes with no lumen (i.e. zippered ER membranes).
A further proof that the *NSP6-labelled round compartments* are made of zippered ER comes from their continuity with the ER itself as shown in the tomograms of Extended Data Fig. 1h-j and Supplementary Movie 1. These images show that the two membranes lining the lumen of a regular ER cisterna come closer and closer and converge into a double-membrane layer with no lumen in between, both in the case of linear and of circular NSP6 structures. Importantly, round ER-zippered membranes are clearly visible also in virus infected cells (Extended data Fig. 8f).
Altogether, our data indicate that the ER zippered by NSP6 can assume a circular or linear shape, and that this occurs not only in the NSP6 transfected cells but also, importantly, in virus infected cells.

The authors now show in a time course the relative speed at which NSP6 deletion mutant vs wt NSP6 to form the round compartments. Although the NSP6 mutant forms NSP6 round compartments faster, it remains unknown whether these NSP6 compartments are a critical path precursor to ROs, an off-target rearrangement of ER membranes, or some sort of ER-associated degradative compartment, which remains a shortcoming of the story because it limits the significance of describing this domain.
We are not entirely sure what the reviewer means by "*an off-target rearrangement of the ER*". If he/she means that the NSP6 compartment is a non-specific consequence of the overexpression of the recombinant NSP6 protein and that it has no functional role, we can exclude that this is the case.
In fact, we show that there are very specific structural requirements for NSP6 to induce the circular and linear zippered ER, and that the circular and linear zippered ER are functionally equivalent since both connect with DMVs and contribute to organizing the NSP3/4 DMVs in NSP3/4/6-expressing cells (Fig. 3c-e, Fig. 6i).
Furthermore, the observation that circular zippered ER membranes are found in virus infected cells (Extended Data Fig. 8f), and thus under conditions where there is no recombinant protein overexpression, argues against an "off-target" ER rearrangement due to protein overexpression.
The functional relevance of the linear and circular zippered ER is best testified by the delta SGF-NSP6 mutant, which is more active in inducing these structures and is also more active in organizing/promoting the growth of DMVs. This mutation in fact evolved in a convergent manner in VOC of SARS-CoV-2 and we show that the gamma variant of SARS-CoV-2 that bears this deletion induces more zippered ER membranes (both linear and circular, see Extended Data Fig. 8f).

The reviewer hypothesizes that the NSP6 compartment might be "*some sort of ER associated degradative compartment*". Though we are not sure which compartment the reviewer alludes to, we can exclude that the NSP6 compartment is related to known ER-associated degradative compartments. We show that the NSP6 compartment does not associate with lysosomes or autophagosomes (Extended data Fig. 1d), and this excludes an ER-phagy related compartment. We can also exclude the recently described non autophagic ERLAD (ER-to-lysosome-associated degradation), as it occurs under the form of single membrane vesicles while the NSP6 compartment consists of double zippered ER membranes.
We show below additional data for the reviewer that argue against a degradative nature of the NSP6 compartment. We posited that if the NSP6 compartment was associated to/destined for degradation it should expand under conditions that inhibit the two major degradative pathways in the cell: the proteasome and the lysosome. However, as shown below in **Figure 2**, the NSP6 compartment contains neither derlin-1, HRD1 or BAP31, three ERAD components, nor does it undergo expansion under treatment with the proteasome inhibitor MG132. Analogously, bafilomycin, which inhibits lysosomal degradation and autophagosome-lysosome fusion, neither induces the accumulation of NSP6 in lysosomes or autophagosomes nor does it induce an expansion of

the NSP6 compartment. Altogether, these data allow us to discard the hypothesis that the NSP6 compartment is a degradation-related/destined compartment.

A second conclusion of the paper is that co-expression of NSP6 even if not exactly co-localized can organize and/or promote formation of NSP3/NSP4 ROs. This does appear to be true, but by what mechanism is not shown.
We thank the reviewer for appreciating our work demonstrating the role of NSP6 in organizing the replication organelle. As for the mechanism, we provide evidence that one of the mechanisms by which NSP6 "*can organize and/or promote formation of NSP3/NSP4"* DMVs involves its ability to zipper the ER membranes (possibly ensuring a more selective protein input from the ER) and to mediate the association of LDs with the RO. We are aware that additional mechanisms may be in place but reaching a complete definition of the molecular mechanisms underlying the biogenesis and growth of the SARS-CoV-2 RO goes beyond the scope of the present manuscript and will be the object of future studies.

I still do not agree with the third conclusion of this paper, which is why I suggested it be removed.
The referee proposes to remove the section on LDs. Although we believe that this section provides insight into one of the mechanisms of action of NSP6, a belief that is likely to be shared by reviewers 2 and 3, we might consider the possibility to remove the section if judged unnecessary.

The data in Fig 4 is not compelling enough to suggest a structural or functional interaction between LDs and NSP6 domains or ROs. The 3 vesicle populations are near each other, but do not appear to overlap, and because all 3 structures are very dense in the ROIs analyzed I suspect the same level of co-localization would be seen in merged images where one of the channels was randomly rotated.
The reviewer casts doubt on the significance of the association of LDs with NSP6 domains or ROs. We would like to reassure the reviewer on this aspect as we have measured thousands of LDs and NSP6 domains and ROs and we have found a very significant effect of NSP6 in increasing this association, as shown in the graphs of Fig. 4f.
However, to address the reviewer's concern we have done what he/she suggested, recalculating all the distances between the NSP3/4 or NSP6 structures and the LDs of our experiments after rotating one of the channels randomly. In doing so, the distances between LDs and the NSP3/4 structures in images with a randomly rotated channel were completely different from those measured in the original images. Indeed, they all increased significantly (at least doubled): the median of the distance between NSP4 and LDs in NSP3/4-expressing cells went from 2.9 (original images) to 6.24 (rotated channel), that between NSP4 and LDs in NSP3/4/6-expressing cells went from 1.3 (original images) to 4.56 (rotated channel), and that between NSP6 and LDs in NSP3/4/6-expressing cells went from 0.4 (original images) to 1.09 (rotated channel), confirming the strength of our data and conclusions.
Nevertheless, we do agree with the reviewer that the image shown in Fig. 4d is not the most representative, so we selected a more representative one.

In a related note, I understand that DFCP1 is being proposed as some relevant LD-ER tether required here for RO biogenesis, but two issues concern me about this conclusion. First, why is the GFP-DFCP1 construct not localized to the ER in the first control panel of Fig 4f, if it is an ER membrane protein? This makes it seem like there something wrong with this expression construct?
The distribution of the DFCP1 expression shown in Fig. 4f is consistent with that reported in the literature (PMID: 11739631, PMID: 18725538, PMID: 22456507, PMID: 24591649, PMID: 25876663, PMID: 26711178, PMID: 28890335). The fact is that DFCP1 is not an ER integral membrane protein but a cytosolic protein that associates with the ER thanks to a motif that we show is also required for its recruitment to the NSP6 structures (Extended Data Fig. 10a, b). Thus, in addition to the ER and a Golgi pool of the protein (indeed, DFCP1 was originally described as a Golgi-associated protein, PMID: 11739631), there is a cytosolic pool that may vary depending on the expression levels. On the contrary DFCP1 is completely cytosolic when mutated in the ER-targeting motif (Extended Data Fig. 10b).

Second, the data showing that GFP-DFCP1 co-localizes upon NSP6 expression around NSP6 vesicles does not show a tethering interaction.
We agree with the reviewer: in fact, we show that DFCP1 is recruited by NSP6, interacts with NSP6 and that this is required for LD consumption by the growing RO, but we do not provide the formal proof that DFCP1 acts as a tether between LDs and the ROs. Hence, we have modified the text accordingly (page 9).

The trend I see throughout the figures is that NSP6 expression causes ER membranes to wrap around NSP6 vesicular domains (by FM and EM) and for example see snapshots for: GFP-DFCP1, Atl2, Rab18, KDELR, VAP and even BODIPY PC.
The reviewer raises the objection that NSP6 does not promote the formation of a distinct ER-derived compartment but induces the ER to wrap around the *NSP6 vesicular domains*. This objection is based on a trend the reviewer envisages in images showing co-labelling of NSP6 with the ER membrane proteins Atl2, KDELR, VAP or the ER-associated proteins DFCP1, Rab18.
Perhaps the reviewer envisages that NSP6 may promote an ER remodelling reminiscent of the OSER (Organized Smooth ER), first described in Snapp et al, (JCB 2003, PMID: 14581454) and caused by the

overexpression of ER resident proteins that promote the ER wrapping by establishing weak interactions through their cytosolic domains.
We can exclude the above possibility for two main reasons. Firstly, we never detect this ER wrapping in the extensive ultrastructural analyses we have performed in NSP6 expressing cells (Fig.1, Fig. 2, Fig. 3 Extended Data Fig. 1, 5, 6, and 8) and **Figure 3** below for further EM images where no ER wrapping can be detected around the NSP6 compartment. Secondly, if the general ER would wrap around NSP6-positive structures one should find general ER markers (i.e. proteins that distribute throughout the ER, such as the luminal ER proteins calreticulin and PDI or calnexin) associated with them, as is the case for OSER (Fig. 3 in Snapp et al.). However, these ER proteins are excluded from the NSP6 compartment as shown in Fig.1 (and **Figure 4** below). Instead, only selected ER markers associate with the NSP6 compartment, for instance, some ER-membrane proteins (KDELR, VAP, Atl2) but not others (ERGIC53, ATF6, Fig.1 Extended Fig. 2). We show below for the reviewer (**Figure 4**) a more complete panel of ER proteins that neither associate with nor are changed by the NSP6 compartment, thus arguing against the ER wrapping around NSP6-positive structures.
As for DFCP1 and Rab18, these are ER-associated proteins that cycle between the cytosol and ER membranes and are selectively recruited by NSP6, but not by mutant forms of it (Fig. 4g, Extended Figure 10 a, b).
Altogether our data indicate that the NSP6 compartment is a distinct compartment emanating from the ER and endowed with a distinct ER membrane composition.

Other minor comments:
- In the rebuttal, the authors say that circular NSP6 domains by FM are taken as proxy throughout the rest of the paper for zippered ER- this is unreasonable as they are clearly two very different kinds of compartments by EM.
This last comment of the reviewer is linked to the first one and stems from him/her considering the "circular NSP6 domains" as clearly very different from the zippered ER. However, as we have explained in detail in the manuscript and above, the combined EM analysis have allowed us to precisely define the ultrastructure of the circular NSP6 domains seen by FM and demonstrate that the circular NSP6 domains correspond to zippered ER membranes that assume a circular shape. That is why we judged it reasonable to take them as proxy for zippered ER.

Referee #2 (Remarks to the Author):

The revised manuscript appears greatly improved and the authors have responded appropriately to my comments. In particular it is acknowledged that there's now at several locations cross reference to data with SARS-CoV-2 infection. The manuscript is very data rich, but well written so that readers are nicely guided through the complex matter. Many details, that probably would deserve entire independent studies, are included in this work, and collectively, this study significantly extends our knowledge on CoV ROs, and the pivotal role that nsp6 has to play.
We thank the reviewer for the positive judgment of how we addressed his/her comments, which were indeed very constructive, and for appreciating our work and our manuscript.

Referee #3 (Remarks to the Author):

>In their revised manuscript, Ricciardi et al. have addressed the points raised by this reviewer by performing additional experiments and quantifying the previously shown qualitative data. The authors have introduced some new tools (e.g., inducible NSP6 expression) to support their previously shown findings and extensively quantified the data shown in the earlier version of their manuscript. These additions have significantly improve the manuscript.
We thank the reviewer for appreciating our work and the effort we put into revising the manuscript that now, thanks also to his/her constructive comments, is very much improved.
*However, there are still few points that need to be addressed via clarification, reanalysis, and new experimentation. In short, there were several quantifications added to better describe the role of NSP6 towards DMV biogenesis. These overall are convincing to suggest the role NSP6 in DMV biogenesis. However, some of these measurements either do not always correlate between the early-lineage NSP6 and the ∆SGF-NSP6 as compared to the DMVs formed in their absence, or they need a separate quantification feature. For example, since the authors define the same ER connectors with the DMVs in the absence or presence of NSP6, the highly zippered ER seen in the ∆SGF-NSP6 may require a new quantification***.**
We thank the reviewer for pointing out the apparent discrepancy between some of the quantified parameters and for identifying an explanation for this discrepancy in the heterogeneity of the measured parameters. Following the reviewer's suggestion, we have now modified some of the "descriptors" of our quantifications (see below for detailed explanation) and resolved the discrepancy.
*In addition, the effect of K22 on DMV biogenesis via its effect on NSP6 is still not sufficiently clarified. The mock control showing the effect of K22 on cells in the absence of NSP6 expression is missing, and the strong effect of K22 on NSP6 relocalisation is not shown for its effect on DMV biogenesis by measuring DMV numbers and morphology***.**

We have addressed the reviewer requests by introducing data on cells treated with K22 in the absence of NSP6 expression (Extended Data Fig. 4c, i) and data on the effect of K22 on DMVs (Extended Data Fig. 7c-f).

More detailed replies are given below to those authors' responses, where I still have comments.<

>The extensive quantifications done by the authors for this part is commendable. The authors have added several quantification measures that are presented mostly in Fig. 3l, m. These quantifications overall imply that DMVs formed in the absence of NSP6 are more connected to the ER and are not homogenous in shape. The expression of NSP6 reduces the number of ER connections which correlates with the formation of more DMVs per connection. Whereas this correlation is shown to work well with the NSP6 from the early lineage SARS-CoV-2, the ΔSGF-NSP6 showed more DMVs per cluster, yet showed more ER connectors per DMV cluster, indicating that reducing the ER connections (or zippered connectors) to the DMV cluster may not be the only NSP6 function that leads to more DMVs per cluster. This is also in contrast to the suggestion from the authors that the expansion of the zippered membranes may favor DMV biogenesis. One possibility could stem from the fact that ER connectors that are quantified in Fig. 3m (from early lineage SARS-CoV-2) are different from the zippered connectors shown for ΔSGF-NSP6, which has to be either quantified differently or should be acknowledged.<

We thank the reviewer for appreciating the extensive quantitative and morphometric analysis we performed, measuring numerous parameters. In these analyses we sometimes compared, as rightly pointed out by the reviewer, parameters that were not perfectly homogenous. This is the case for the "connections" quantified in Fig. 3m that in fact referred mostly to tubular connections for NSP3/4-expressing cells or mostly to zippered connections (which we named connectors) for NSP3/4/NSP6-expressing cells. This may have generated the mismatch noted by the reviewer. In revising the manuscript, we have amended this aspect by specifying the type of measured connections, whether tubular or zippered.

>The authors have made substantial efforts to describe the qualitative differences observed in DMVs in the presence or absence of NSP6 into quantitative measurements. Particularly interesting is the increase in the number of DMVs seen in the clusters in the presence of NSP6 and ΔSGF-NSP6. These additional data have improved the manuscript and better describe the effect of NSP6 on DMV biogenesis.
However, there are some details that need attention. As described in the comment above, some quantified features do not always fully correlate with the function of NSP6 towards increasing the number of DMVs in the cluster or inducing homogenous size, e.g., the number of ER connectors. This is either due to the lack of some measurements (e.g., DMV diameter in the ΔSGF-NSP6) or using the same measurement for the ER connectors in presence or absence of NSP6. This should be clarified or acknowledged better.
As mentioned above, we realized that comparing the number of "connections" established by DMVs in the absence and presence of NSP6 might have been misleading as they are not of the same type, as pointed out by the reviewer. Indeed, they are mainly tubular connections in the absence of NSP6 and zippered ER connections (which we named connectors) in the presence of NSP6. We were aware of this difference and in fact we used the term "connections" in Fig. 3m, when comparing NSP3/4 vs NSP3/4/6-expressing cells. By contrast, we used the term "connectors" (i.e. zippered ER connections) when we compared the NSP3/4/6 wt and NSP3/4/6 deltaSGF (extended data Fig. 8c). However, we realized that this subtle semantic difference was insufficient to avoid confusion. In the revised manuscript we clarified this point and, following the reviewer's suggestion, we made a distinction between tubular ER connections and zippered ER connections and we also measured the DMV diameter in ΔSGF-NSP6. The new data are included in Fig. 3 k-m and in Extended data Fig. 8.
Fig 3 shows that 1: NSP6 decreases the number of tubular connections and promotes the formation of zippered connections; 2: the ratio of DMVs per tubular connection (in NSP3/4-expressing cells) is five-fold lower (3 vs 15) than the ratio of DMVs/zippered connections (in NSP3/4/6-expressing cells). Fig. 3m and Extended data Fig. 6e-j also show that the DMV shape is more regular, the DMV diameter is more homogeneous, and the DMV number per cluster is higher in ΔSGF-NSP6 than in NSP6-expressing cells.
Altogether, our quantitative analysis shows that the main role of NSP6 is to provide the DMVs with zippered and, as such, more selective connections to the ER and to reduce the number of "tubular" (less selective) ER connections. Thus, it is the shape (i.e. the zippering) of the ER connections that makes the difference and that correlates "with the function of NSP6 towards increasing the number of DMVs in the cluster or inducing a homogeneous size". This correlation holds for ΔSGF-NSP6 that makes more numerous ER-zippered connections and, hence, renders the vesicles in the DMV clusters more numerous and more homogeneous.
We thank the reviewer for highlighting this apparent inconsistency that we have now resolved. We have accordingly modified the text of the revised manuscript (page 6 and 7).

The authors should also comment if the diameters of DMVs uniformly decrease to compensate the increase in its number as seen with early lineage NSP6 (Extended data Fig. 6f), by including this data for the ΔSGF-NSP6. If so, the increased "DMV expansion" might not be related to the role of NSP6 in DMV biogenesis.
We agree with the reviewer that the term "DMV expansion" might be misleading as it could indicate increase in DMV size, so we have eliminated it from the text. In this context, we would like to point out that NSP6 has a predominant qualitative effect on DMVs (manifesting in more regular shape and size as specified above), but also has a quantitative impact on DMVs (increase in DMVs number per cluster). The reviewer correctly noticed that this increase in the number of DMVs per cluster induced by NSP6 is paralleled by a decrease in their size. However, these two processes happen with different magnitude and do not seem to compensate each other. With NSP6 the vesicle diameter decreases by 16% (from 80.8 to 67.5 nm), while vesicle number increases in a

more substantial manner (by 52%). This suggests that NSP6 promotes a net increase in DMVs area in addition to making DMVs more numerous and more homogeneous. This notion is further supported by our findings on ΔSGF-NSP6. Following the reviewer's indication, we measured the diameter of DMVs in ΔSGF-NSP6/NSP3/NSP4–expressing cells and found that the average diameter was not different from that of DMVs in NSP6/NSP3/NSP4–expressing cells (68.5 vs 67.5 nm). The significant differences we found were in the size distribution of DMVs and in their number: the size distribution was more homogenous and the number of DMVs was higher (doubled) in the presence of ΔSGF-NSP6 compared to early lineage NSP6 (Extended data Fig. 8 c-e and legend). As a consequence, DMV clusters were significantly bigger and the overall area occupied by DMVs was higher in the presence of ΔSGF-NSP6 as compared to early lineage NSP6.

In addition, the authors showed that K22 causes a change in the localization of NSP6, but the impact of K22 on DMV biogenesis (number and morphology) is missing. This data is desirable to fully understand the contribution of NSP6 towards DMV biogenesis, given the strong impact of K22 on NSP6 localisation.< This was an excellent suggestion. We performed EM analysis of cells expressing NSP3/4/6, which were exposed to K22. It revealed that DMV clusters contained a significantly lower number of vesicles (Extended data Fig. 7c-f) compared to the control cells. Vesicles in such clusters exhibited a less regular shape and lost zippered connections to the ER membranes. Instead, more numerous tubular connections of DMVs with ER were detected (Extended Data Fig. 7f). This suggests that the ability of K22 to perturb the NSP6 compartment translates in a failure of NSP6 to coordinate DMV biogenesis.

>*These results suggest that the dimer and oligomer formation between NSP6 molecules can still occur in the absence of the C-terminal region of NSP6 that harbors the amphipathic helix. This should be reflected in the model (Extended Fig 11) where NSP6 dimers are linked via the C-terminal residues.*< We thank the reviewer for his/her comment. We have amended the model to make it consistent with our dimerization data. (Extended data Fig. 11).

>*Though the results depicting the change in localization of NSP6 puncta close to the nuclear envelope is shown clearly, the suggestion that this led to the zippering of the nuclear envelope is rather premature. The images (Extended data Fig. 4 f-h) showing the described zippering of the nuclear envelope are not clear enough to make this claim.*
We have introduced clearer images of our EM analysis in Extended data Fig. 4 f-h. It is now visible that the zippered membranes induced by NSP6 upon K22 treatment host nuclear pore structures, thus unequivocally demonstrating their nuclear envelope nature. As a control we have also added images of cells treated with K22 but not expressing NSP6 (Extended data Fig. 4 i): under this condition no NE change (like zippering) is visible as compared to untreated cells, demonstrating the NE zippering induced by K22 is mediated by NSP6.

This should be supported further using an ER membrane marker that associates with NSP6 using immunofluorescence staining (Fig. 1j, Extended data Fig. 2).
As requested by the reviewer, we analyzed the impact of K22 on the distribution of an ER membrane marker populating the NSP6 structures, i.e. VAPA. Once again, in the absence of NSP6, K22 treatment did not alter the distribution of this marker, while the same marker was found with NSP6 in the elongated structures corresponding to the NE (Extended data Fig. 4c).

In addition, the mock control for the effect of K22 on cells in the absence of NSP6 expression is missing. This is important to rule out the possibility that K22 alone can induce changes to the ER membranes close to the nuclear envelope or nuclear envelope itself.
We thank the reviewer for pointing out the need to show control cells treated with K22. We had indeed already performed this analysis and we have now introduced images of cells not expressing NSP6 treated with K22 in Extended data Fig 4c, i. In agreement with the above EM and IF results, an ER marker such as VAPA (which distributes in the ER/NE) is not altered by K22 treatment in cells not expressing NSP6, confirming that the remodelling of the ER/NE caused by K22 depends on the presence of NSP6.

>*In the final model, NSP6 dimers appear to interact via N-term to C-term, which is contrary to the data shown in the revised manuscript where NSP6 dimers still interacted in the absence of the loss of C-term residues harboring the amphipathic helix. The authors should harmonise their model accordingly.*<
We thank the reviewer for his/her comment: we have harmonized the model in Extended data Fig. 11 with our data.

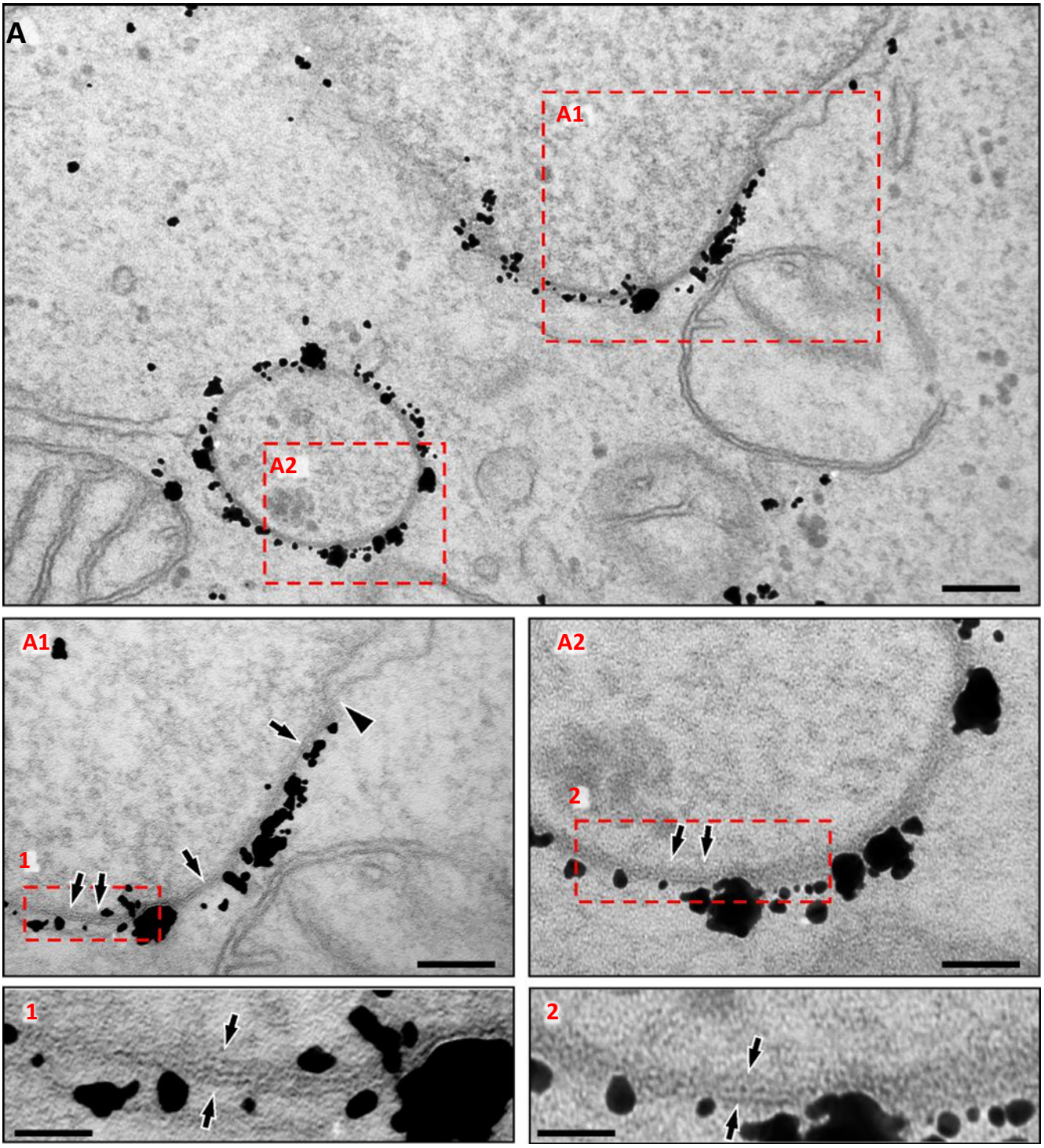

Figure 1. The NSP6 compartment is made of zippered ER membranes. A, High magnification image of linear (A1) and circular (A2) zippered ER membranes. **A1,** Magnification of boxed area A1 in panel A. Arrowhead indicates the place where two opposite membranes of the nuclear envelope join into the zippered domain, which is heavily labelled with NSP6-associated gold particles. Arrows indicate area of the zippered domain where two attached membranes can be clearly seen. Boxed area 1 (magnified in 1) demonstrates two attached membranes. **A2,** Magnification of boxed area A2 in panel A showing part of the circular zippered ER domain. Arrows indicate areas of the zippered domain where two attached membranes can be clearly seen. Boxed area 2 (magnified in 2) shows two attached ER membranes (arrows). Scale bar: 200 nm (A), 70 nm (A1, A2), 18 nm (1, 2).

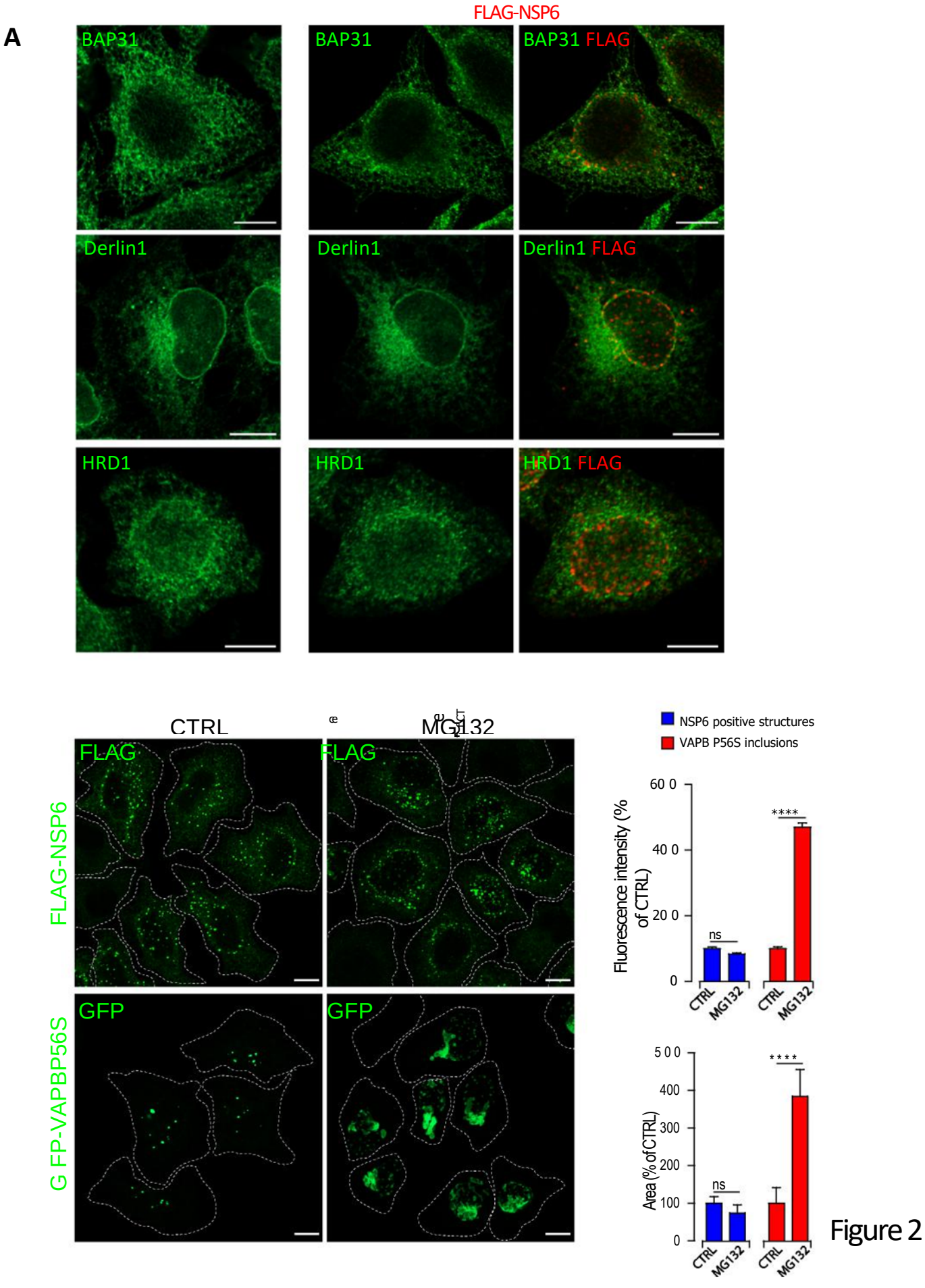

Figure 2

nature portfolio

C

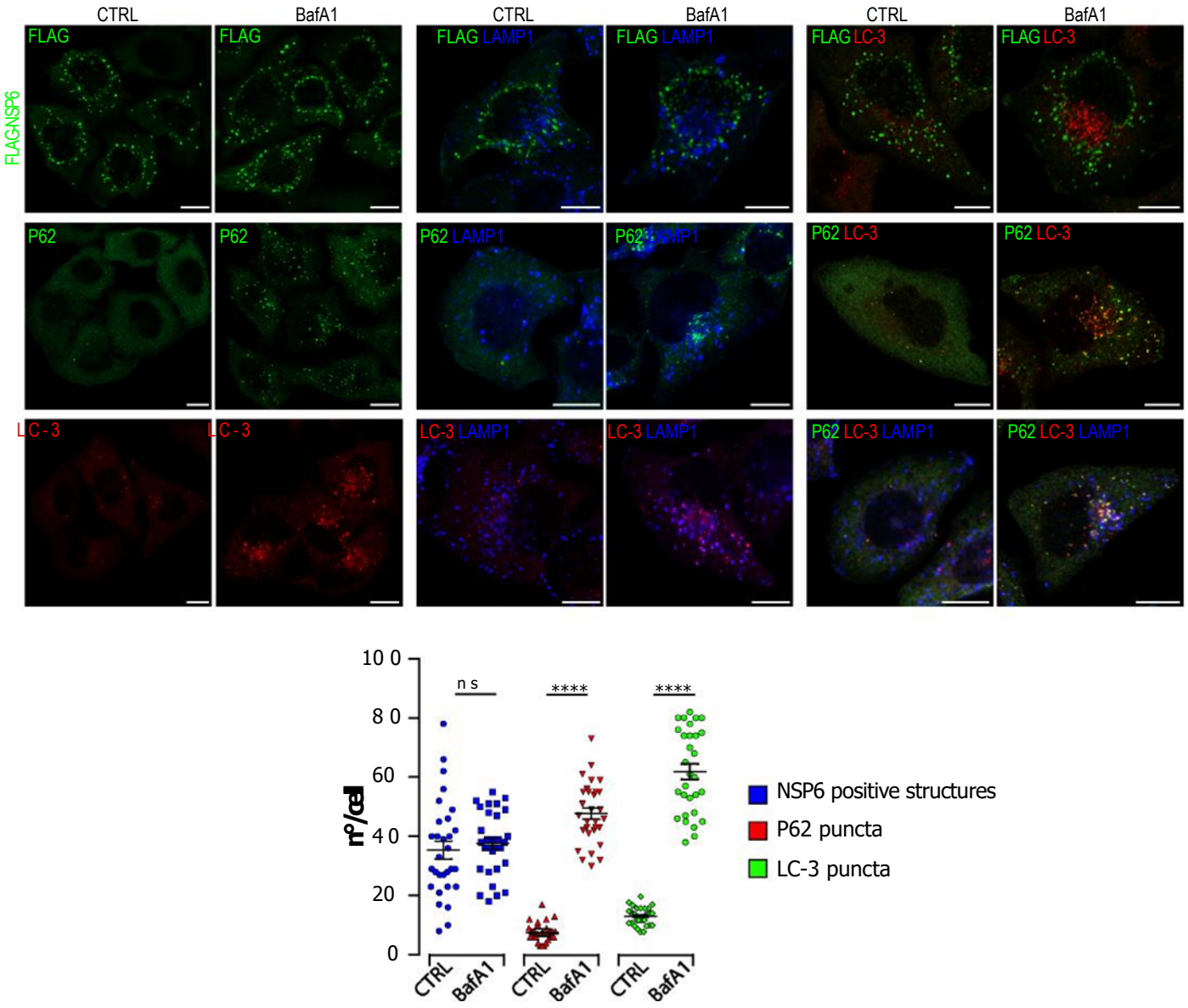

Figure 2. The NSP6 compartment is not a degradative compartment. A, The NSP6 compartment does not contain ERAD components like BAP31, Derlin-1 and HRD1. HeLa cells expressing NSP6 protein (red channel, right panels) or not (left panels) were stained with BAP31 (top) or Derlin-1 (middle) and HRD1 (bottom) in green. **B,** The NSP6 compartment does not expand upon proteasome inhibition. GFP-VAPB-P56S, a mutant form of VAPB inducing ER inclusions, was used as a positive control. VAPB inclusions expand upon proteasome inhibition with MG132 (10 µM, 4 hrs) in agreement with published reports (PMID 22611258, 24252306, and 25409455). The graphs report the mean fluorescence intensity (top) and the average size of NSP6 or VAPB-P56S structures in control (CTRL) and MG132-treated HeLa cells. Values are plotted as percentage of control (mean ± SEM), n = 30. **** $p < 0.0001$, Mann-Whitney test; ns= not significant. **C,** The NSP6 compartment is not a degradative compartment connected with the autophagosome-lysosome pathway. The NSP6 compartment does not undergo expansion upon inhibition of lysosome degradation by bafilomycin (BafA1, 200 nM, 3hrs). p62 and LC-3 were taken as positive controls since the p62 and LC3 labelled structures undergo expansion upon inhibition of lysosomal degradation. p62 and LC3, but not NSP6, colocalize with the lysosomal marker LAMP1. Scale bars, 10 µm. The graph shows the number of NSP6, P62 or LC-3 structures in control (CTRL) or upon BaFA1 treatment. Values are plotted individually with means ± SEM. n = 30. **** $p < 0.0001$, Mann-Whitney test; ns = not significant.

Figure 2

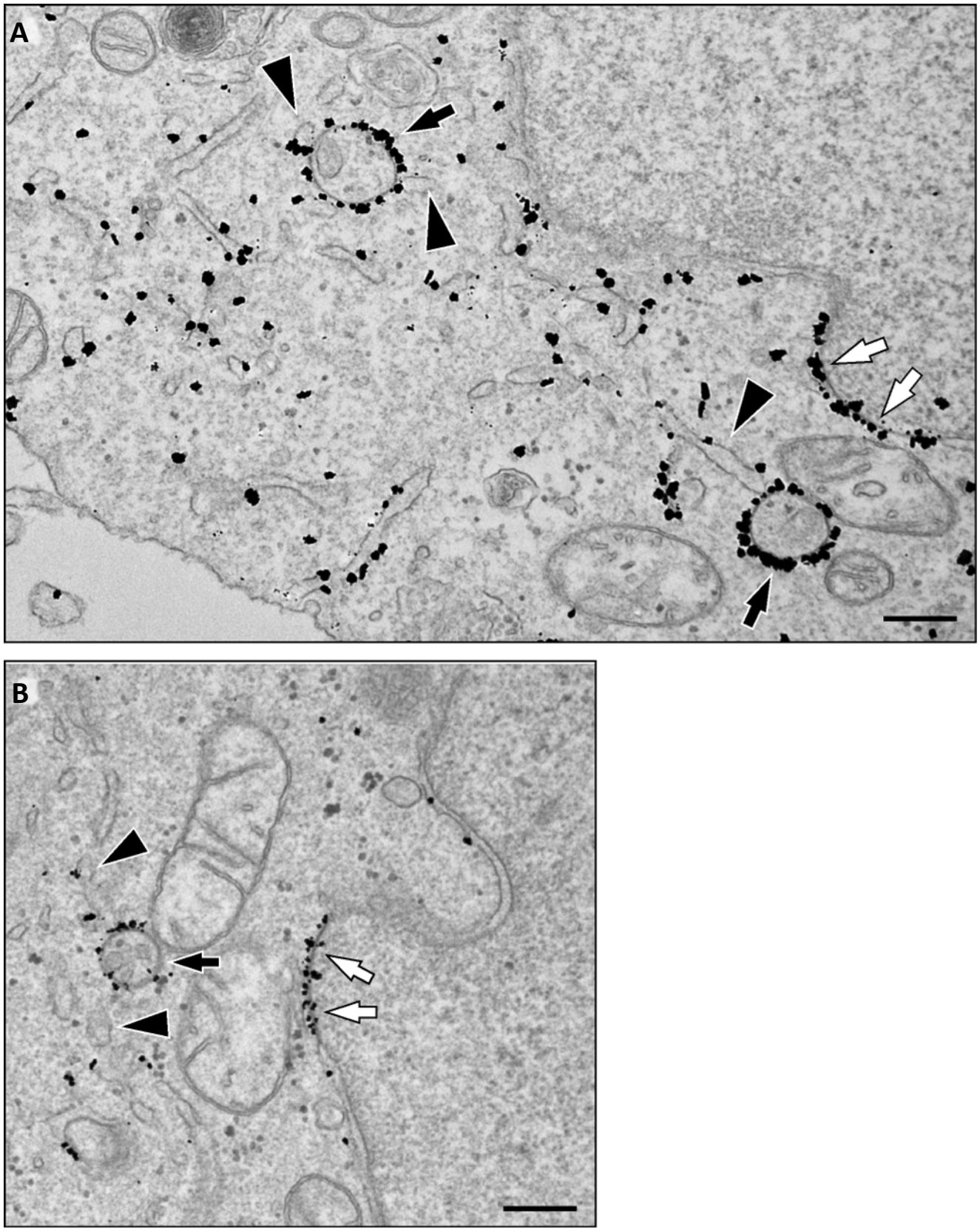

Figure 3. Regular ER is not wrapped around circular NSP6-positive zippered ER. A, B, Representative low magnification EM images of HeLa cells expressing HA-NSP6 immuno-gold labelled for HA. Black arrows in A and B indicate circular zippered ER domains heavily decorated by gold particles associated with NSP6. White arrows show linear zippered domains of the nuclear envelope, which forms part of the ER. Note that regular ER profiles (arrowheads) do not wrap around the circular zippered ER.

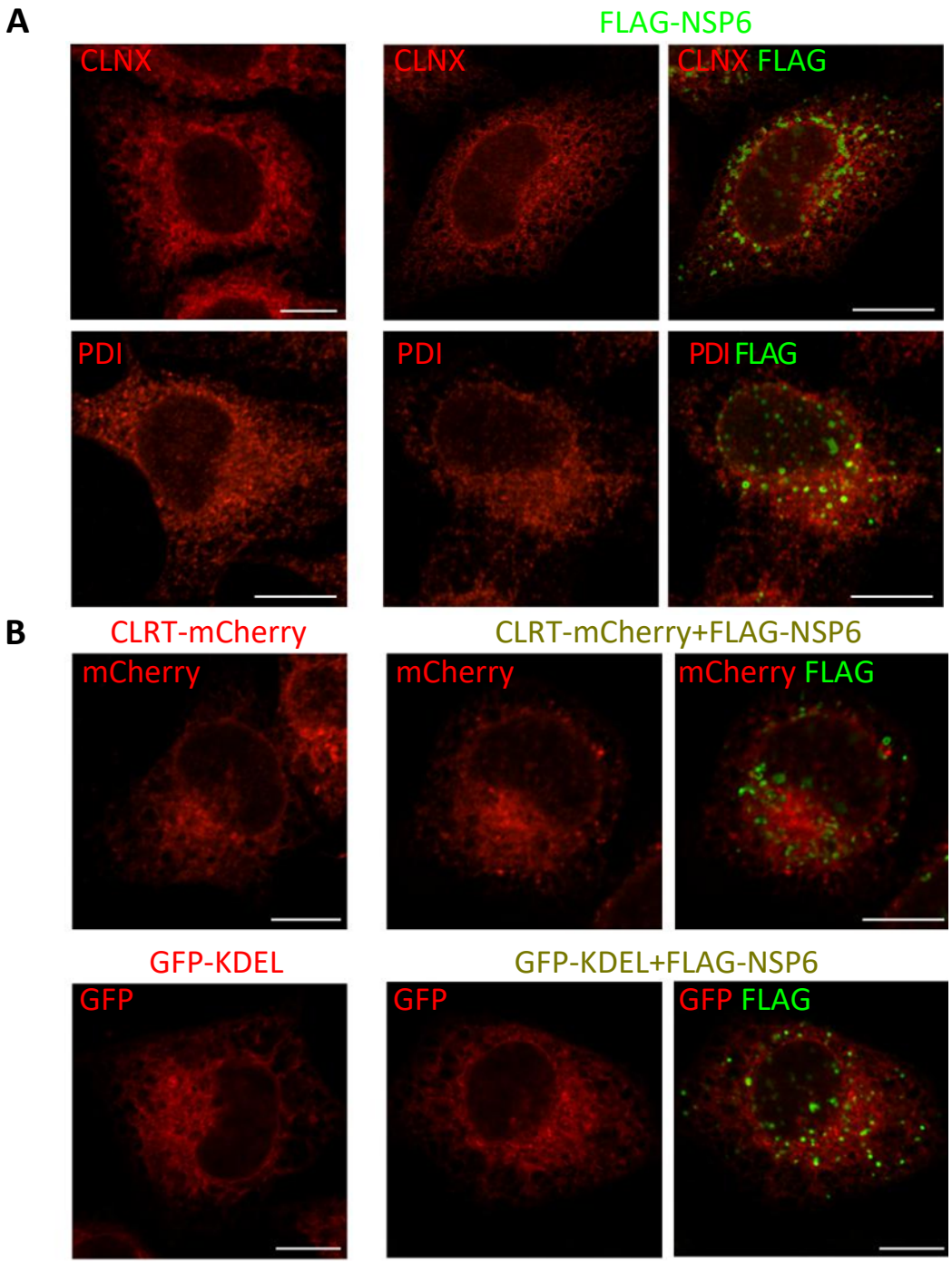

Figure 4. Regular ER is not wrapped around circular NSP6-positive structures. Immunofluorescence images of endogenous (**A**) or transfected (**B**) ER markers in control (left panels) or NSP6-expressing HeLa cells **A,** Endogenous Calnexin (CLNX, red) and PDI (red) were acquired in the absence (left) or in the presence of FLAG-NSP6 (green). **B,** Hela cells were transfected with Calreticulin-mCherry (CLRT, red, top panels) or with GFP-KDEL alone or together with FLAG-NSP6. Note that none of the analyzed ER proteins show any degree of co-localization with the NSP6 compartment. Scale bars, 10 µm.

Figure 4

Reviewer Reports on the Second Revision:

Referees' comments:

Referee #1 (Remarks to the Author):

The authors have clarified most of my concerns regarding whether NSP6 is a precursor and relevant compartment that contributes to the organization of the NSP3/4 domain. I also concede that the zippered flat and zippered round compartments may be similar enough. As it stands these data represent a significant discovery in the biogenesis of a virus on the ER membrane.

I remain unconvinced by the association with the LDs and think the paper would be stronger without this weaker data. I might have been convinced had data been included showing representative examples of which images were measured before and after rotation, what size ROIs were used, and some kind of statistics showing that these data were performed in a reproducible and significant way.

Referee #3 (Remarks to the Author):

In this re-revised version of the manuscript the authors have properly addressed my remaining comments. Although two recent studies have shown that nsp3-4 of SARS-CoV-2 suffices to induce DMVs and the important role of DFCP1 in SARS-CoV-2 replication, respectively, the present study provides novel information on the role of nsp6 in RO formation of this virus. I have no further comments.

Author Rebuttals to Second Revision:

Referee #1 (Remarks to the Author):

The authors have clarified most of my concerns regarding whether NSP6 is a precursor and relevant compartment that contributes to the organization of the NSP3/4 domain. I also concede that the zippered flat and zippered round compartments may be similar enough. As it stands these data represent a significant discovery in the biogenesis of a virus on the ER membrane.
We thank the reviewer for recognizing the importance of our results.

I remain unconvinced by the association with the LDs and think the paper would be stronger without this weaker data. I might have been convinced had data been included showing representative examples of which images were measured before and after rotation, what size ROIs were used, and some kind of statistics showing that these data were performed in a reproducible and significant way.

As we specified in our previous response to the reviewer, we applied this rotation to at least 30 different cells per condition and we found that the distances between LDs and the NSP6/NSP4 structures in images with a randomly rotated channel were completely different from those measured in the original images. Indeed, they all increased significantly (at least doubled), confirming the strength of our data and conclusions. The significance of the difference between the distances measured in the original and rotated images was evaluated by Kruskal-Wallis test with Wilcoxon posthoc and Bonferroni correction, and shows significant differences (p values < 0.0001).

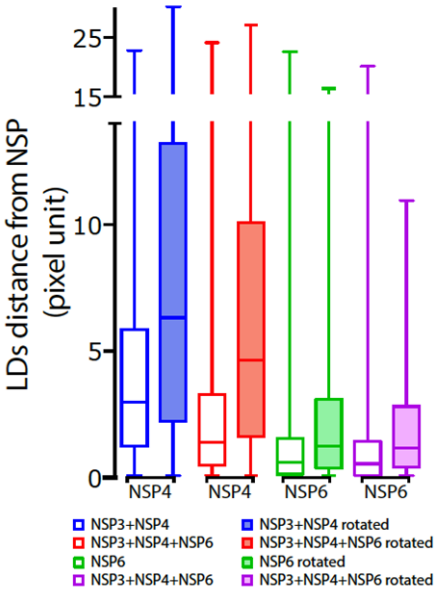

Now the referee is asking for representative examples measured before and after rotation.

We provide below as an example the image of Fig. 4d (Fig. 4a of the revised version), which clearly shows that the distances between LD and NSP structures measured in the original image are completely different (and invariably shorter) than those measured in the rotated images.

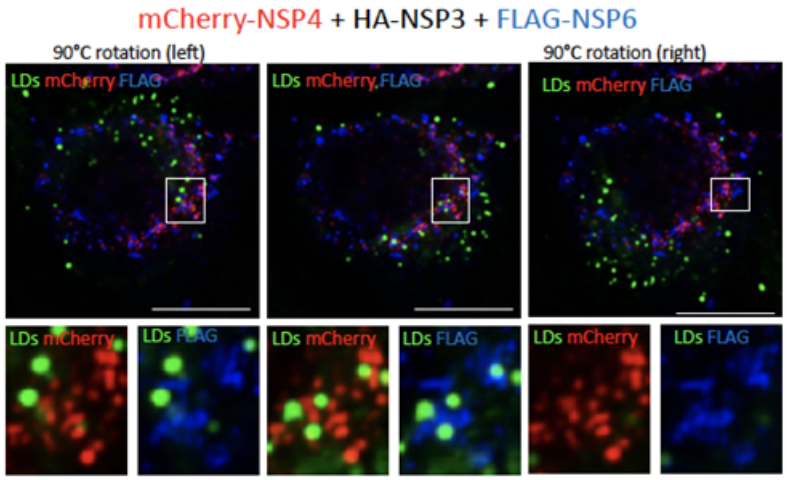

NSP6/LD distance		4.629	**0.332**	1.551
NSP4/LD distance	5.087	**0.711**	2.211	

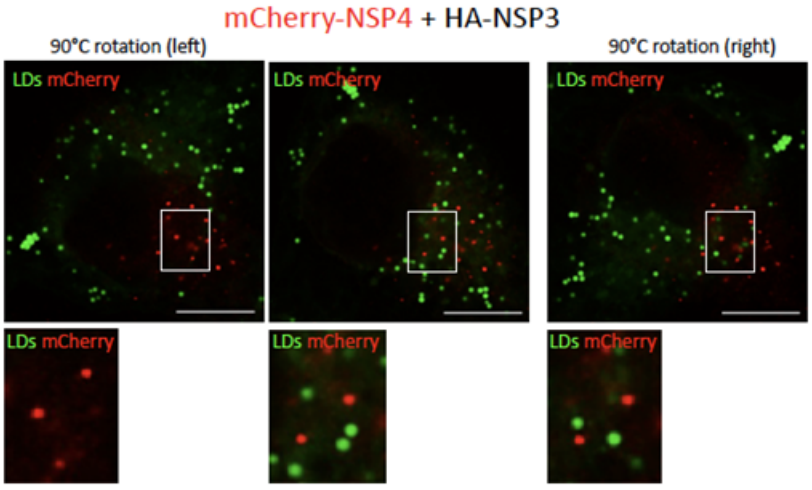

NSP4/LD distance	7.111	**3.957**	8.520

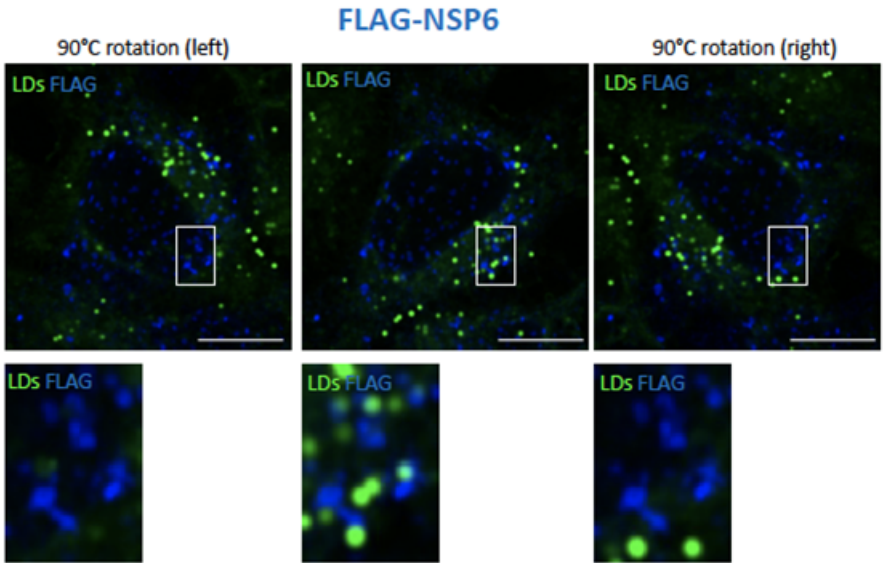

NSP6-LD distance	1.715	**0.361**	6.9485

As a further proof that the LD- RO distances we measure are meaningful and not random, we are showing below the results obtained using the plugin Shuffle of the software we used to measure the LD-RO distance (DIANA). Shuffle applies a method from spatial statistics analysis to object-object distances measured in IF. The shuffle function can redistribute the objects in a uniform manner within the whole image: shuffled images are generated, and for each of these images the distances between objects of the randomized channel to the closest object in the second channel from the original image are computed. The cumulative distribution of the distances is plotted and represented as the mean (red curves) flanked by 95% confidence intervals of the results (green curves). In parallel, observed distances between objects from the non-randomised original images are measured and plotted on the same graphic (blue curves). If the distribution of the distances from experimental images (blue line) falls outside the confidence interval of the distance distribution obtained for shuffled images in which object locations are random (green lines), one concludes that there is less than 5% chance ($p<0.05$) that the observed distances are random and thus the measured distance is considered as statistically significant.

Below is the graph obtained applying the function Shuffle to the cell shown in Fig. 4 for the “NSP6 objects” and “LD objects” in NSP3-NSP4-NSP6 transfected cell, showing that the measured distances (blue line) are significantly different from random distances (green lines) .

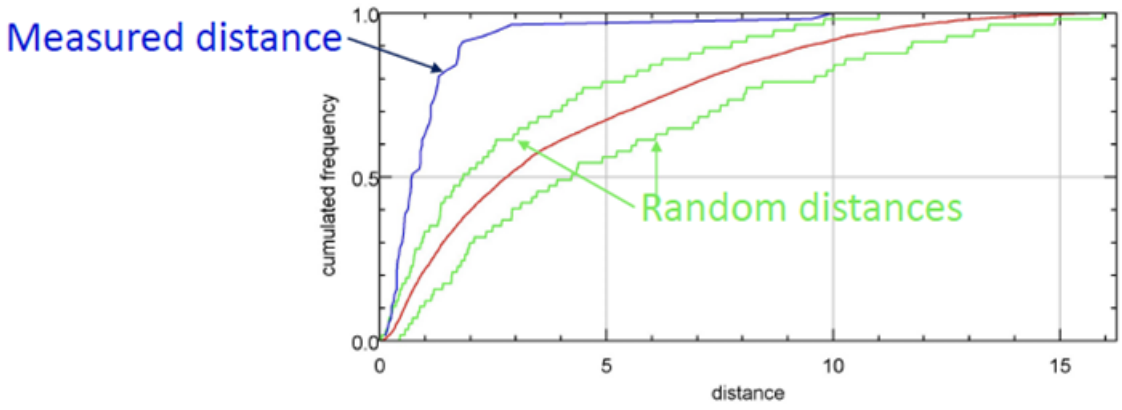

.

Regarding the reviewer's question, what size of ROI were used, we now realize (from the request to specify the size of the ROI used) that there has been an original misunderstanding as the reviewer assumes that we measured LD-RO distance only in selected ROIs. However, we never mentioned that we used any ROI since we measured the LD-RO distances in the entire cell for hundreds of cells and thousands of lipid droplets. To avoid any possible misinterpretation, we now clarify in Methods and the legend to Fig. 4 that the distances were measured in the entire cell and not in a selected ROI. Our statistical analysis thus takes into account thousands of LDs overall from hundreds of cells and in fact returns extremely significant differences in the differences measured: $p = 0.00014$, analysed by Kruskal-Wallis test with Wilcoxon posthoc and Bonferroni correction.